Synchronization of Markovian Jump Neural Networks for Sampled Data Control Systems With Additive Delay Components:Analysis of Image Encryption Technique

Tamil Thendral M[1], Ganesh Babu T.R[2], Chandrasekar A[3], and Yang Cao[4]

[1]Anna University Chennai
[2]Muthayammal Engineering College
[3]Sona College of Technology
[4]Southeast University

March 07, 2024

Abstract

In an modern world, image encryption played an vital role to prevent our data from illegal abuser entre. Based on this, in this paper the Markovian jump neural networks for synchronization of sampled-data control systems with two additive delay components are used on the looped functional method and its direct application is applied in image encryption. On the basis of generalized Lyapunov functional approach involves the states information such as x(tk) and x(tk+1) with few slack variables and a tuning parameter are introduced . Furthermore, the sampled-data controller is designed to contain both the present and delayed state information, thereby enhancing the control performance and design flexibility. Finally by using the new technique, the several examples are highlighted in the numerical section and also the effectiveness of an image encryption is studied.

Hosted file

`image synchronization.tex` available at https://authorea.com/users/416382/articles/709982-synchronization-of-markovian-jump-neural-networks-for-sampled-data-control-systems-with-additive-delay-components-analysis-of-image-encryption-technique

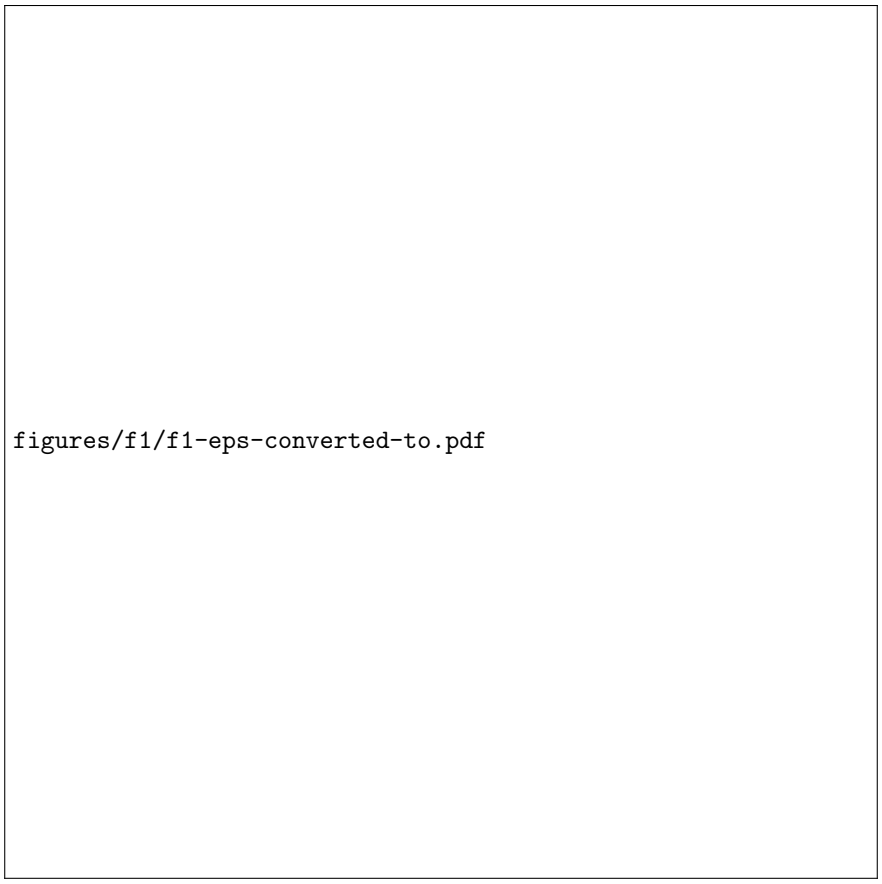

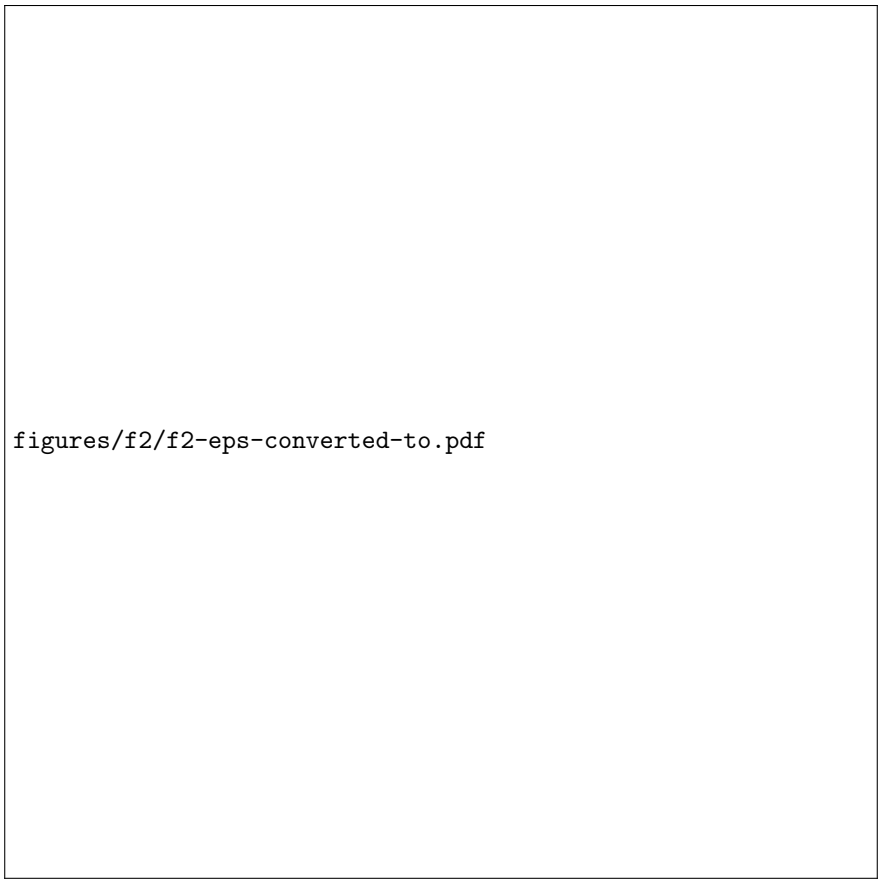

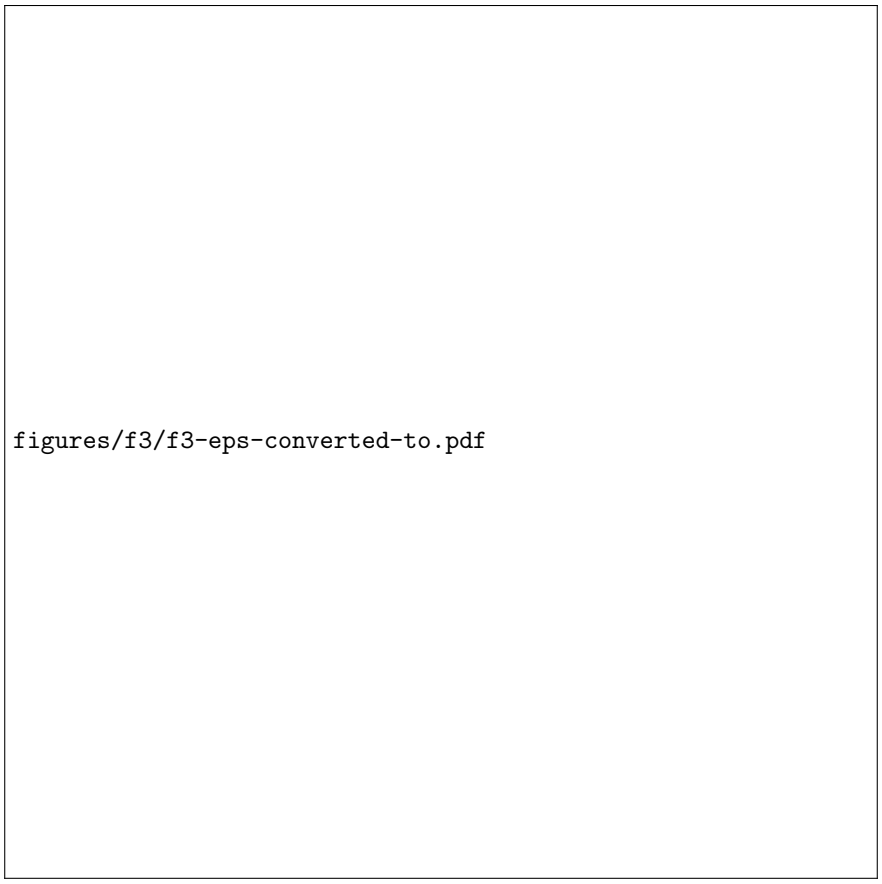

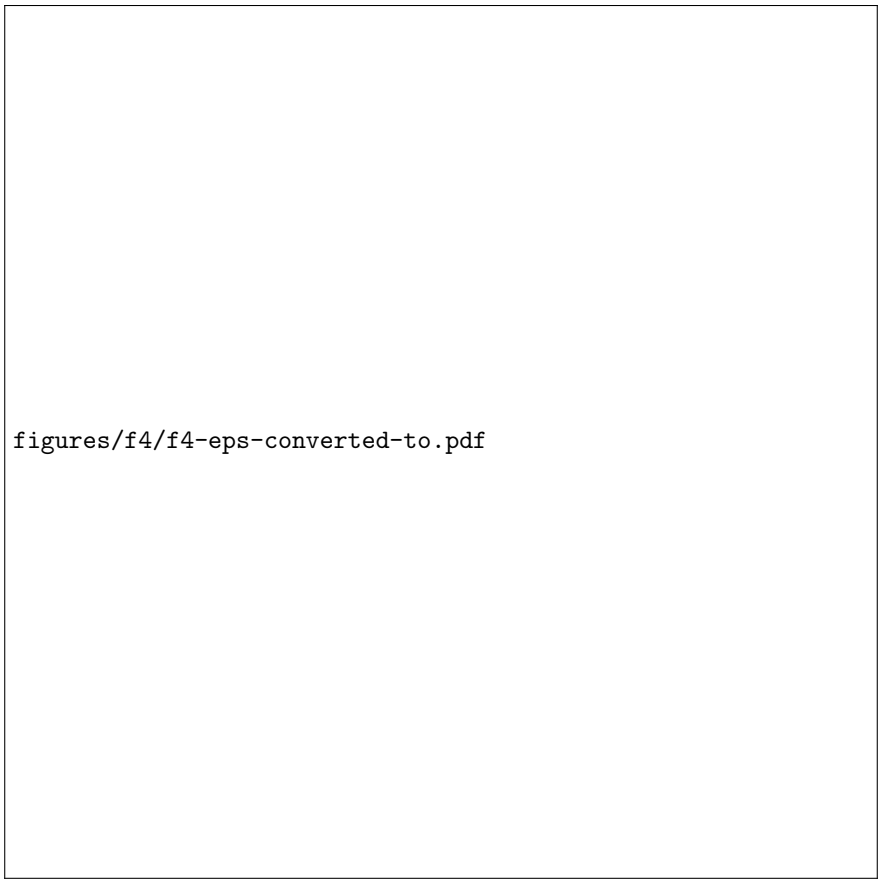

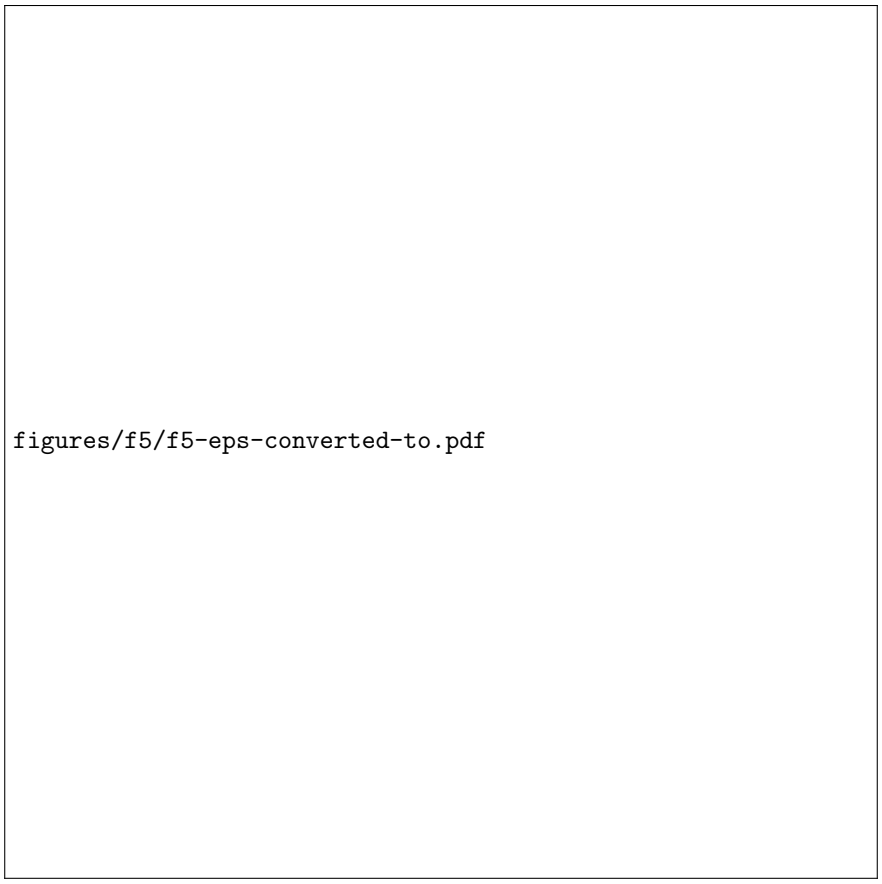

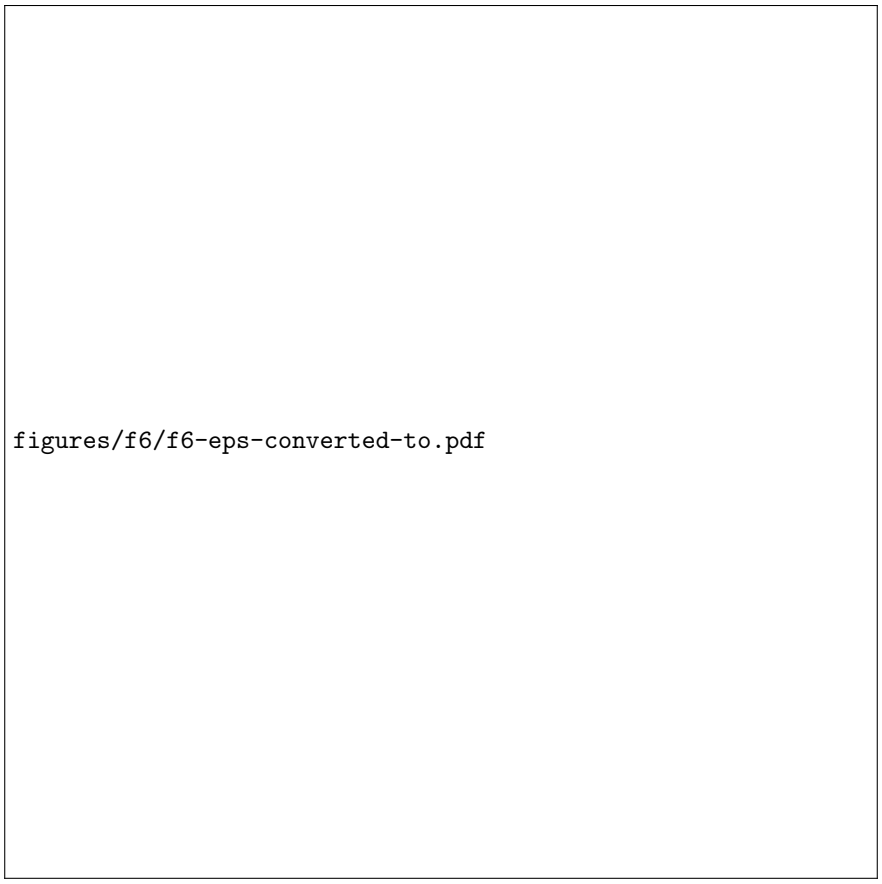

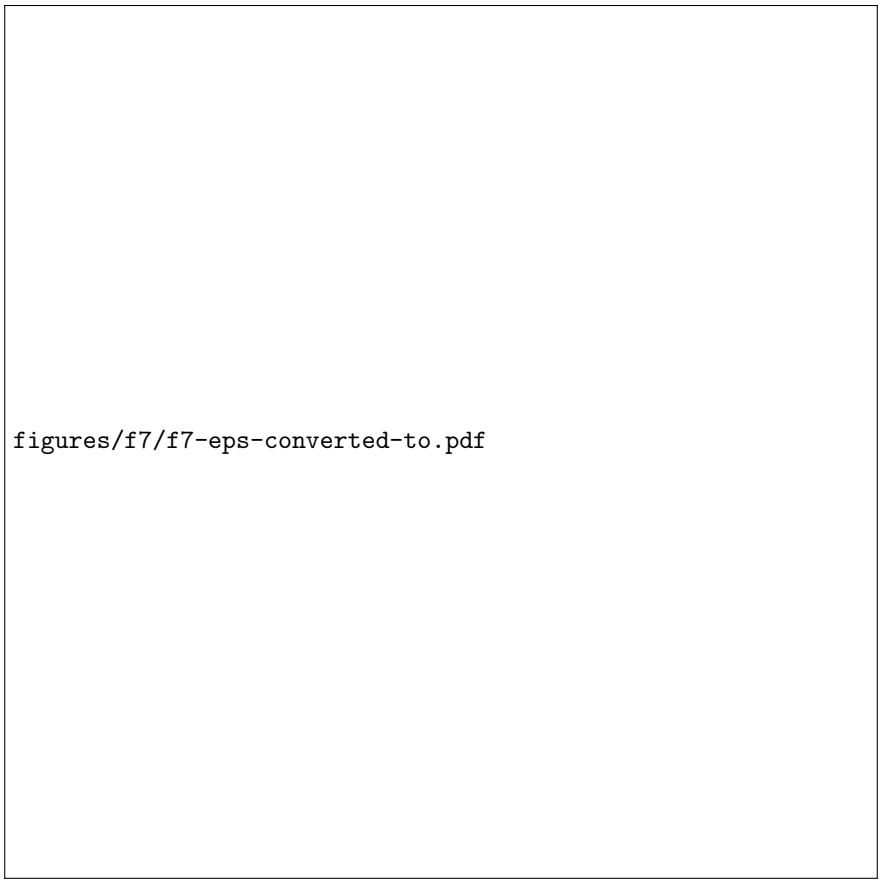

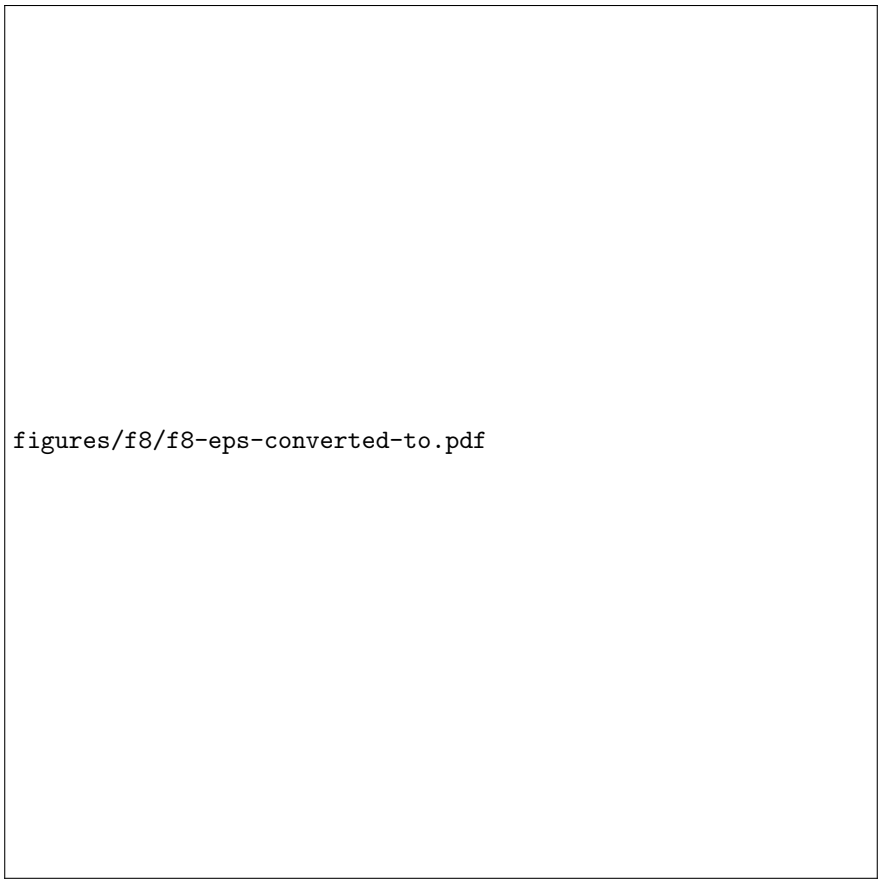

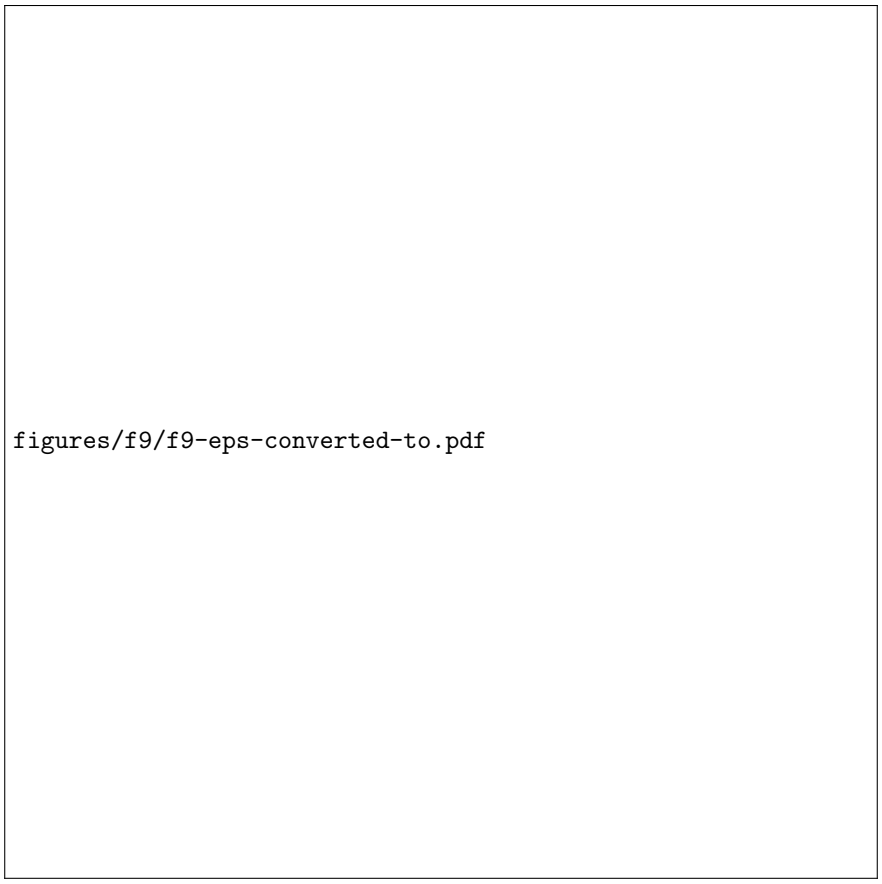

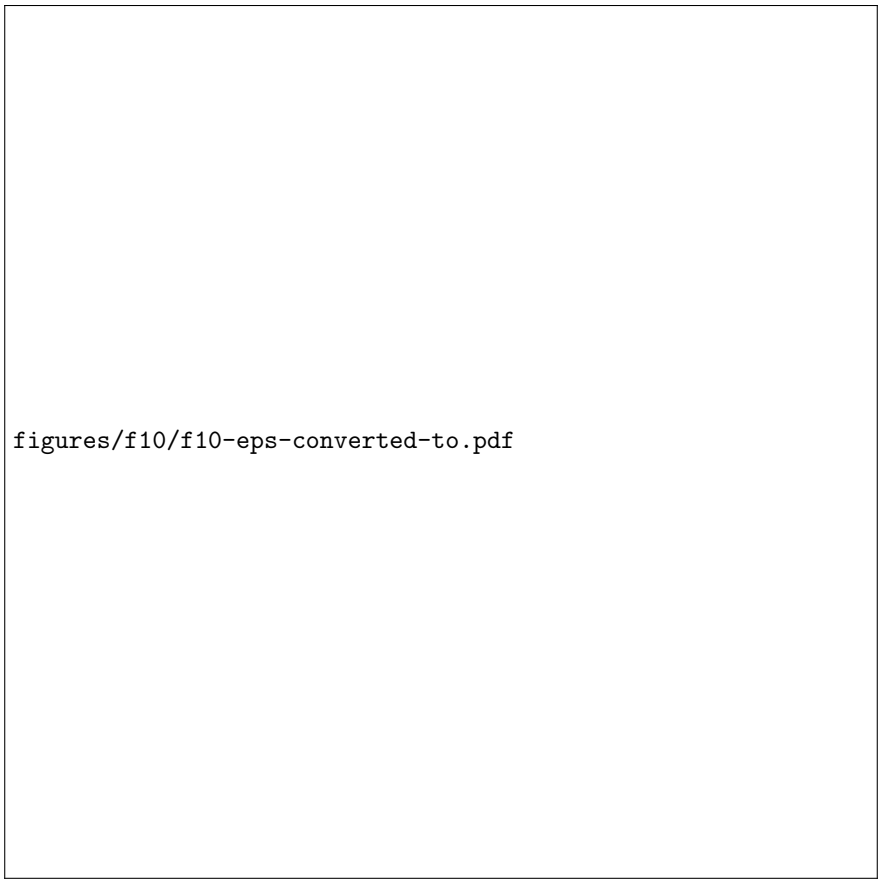

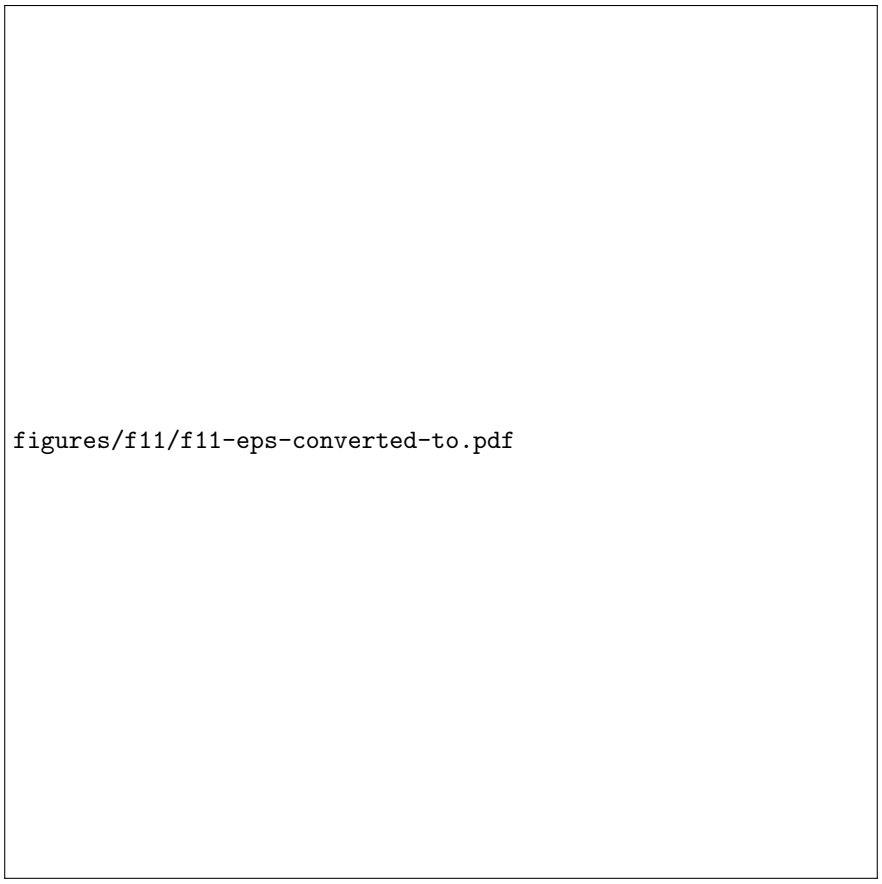

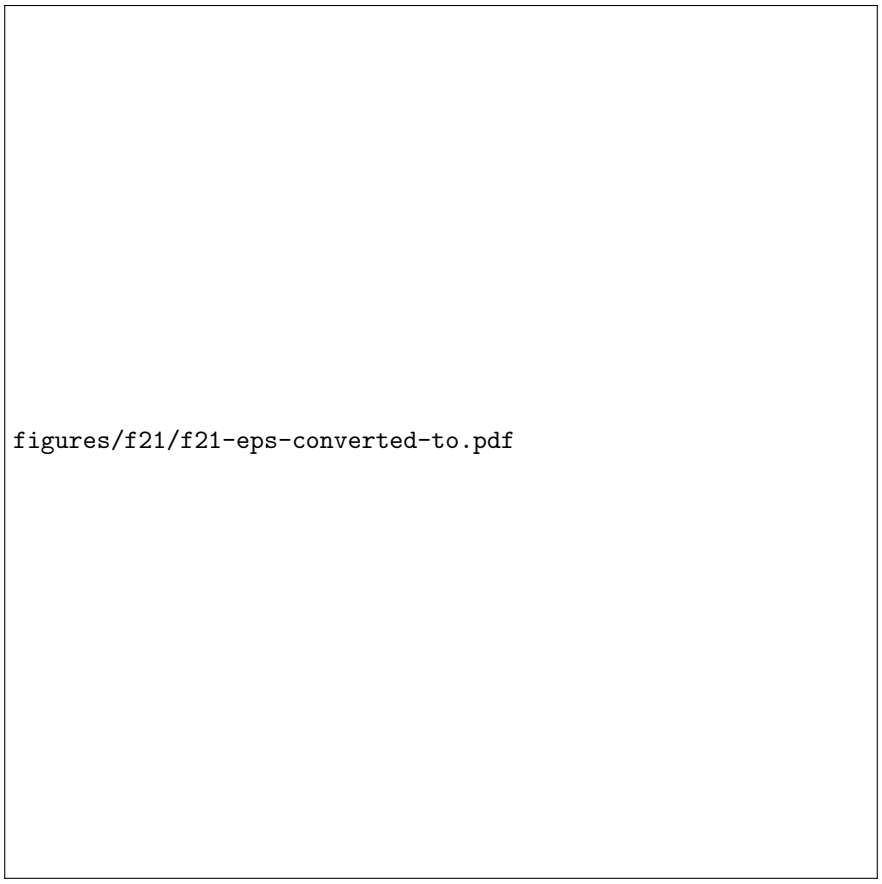

Synchronization of Markovian Jump Neural Networks for Sampled Data Control Systems With Additive Delay Components:Analysis of Image Encryption Technique [1]

M. Tamil Thendral[†], T.R. Ganesh Babu[‡], A. Chandrasekar[*], Yang Cao[**]

[†]Research Scholar, Department of Computer Science and Engineering, Anna University, Chennai 600025, Tamil Nadu, India

[‡]Department of Electronics and Communication Engineering, Muthayammal Engineering College, Rasipuram 637408, Tamil Nadu, India

[*]Department of Mathematics, Sona College of Arts and Science, Salem - 636005, Tamil Nadu, India

[**]School of Cyber Science and Engineering, Southeast University, Nanjing 210096, China

Abstract: In an modern world, image encryption played an vital role to prevent our data from illegal abuser entre. Based on this, in this paper the Markovian jump neural networks for synchronization of sampled-data control systems with two additive delay components are used on the looped functional method and its direct application is applied in image encryption. On the basis of generalized Lyapunov functional approach involves the states information such as $x(t_k)$ and $x(t_{k+1})$ with few slack variables and a tuning parameter are introduced . Furthermore, the sampled-data controller is designed to contain both the present and delayed state information, thereby enhancing the control performance and design flexibility. Finally by using the new technique, the several examples are highlighted in the numerical section and also the effectiveness of an image encryption is studied.

Keywords: Synchronization, looped functional method, Markov jump systems, Linear matrix inequality, Sampled-data control.

1 Introduction

During the last few decades, synchronization plays an important role in the development of computer and communication technology. Since Pecora and Carrol [1] initially introduced the drive response systems, then it is extended for chaos synchronization and have been extensively attracted in many application such as biological systems, traffic systems, pathological states in the brain, secure communication [2,3], pattern identification [4], image cryptosystem [5], and so on. Many tentative study and

[1]Corresponding authors-E-Mail addresses: chandrudhana28@gmail.com (A. Chandrasekar), caoyeacy@seu.edu.cn (Yang Cao)

computer graphics of chaotic synchronization in unidirectional coupled external cavity semiconductor lasers have shown the existence of delay time between the drive and response laser's intensities. Now a days, synchronization plays an vital role in secret communication and other nonlinear fields. Further, the synchronization of neural networks have been applied with sampled data control, time-delay, fuzzy control and so on. Therefore, the investigation of synchronization for neural networks plays a great importance.

It should be noted that, while executing artificial neural networks time-delay is often came across in real applications. Further, the signal transmissions among neurons and the finite switching speed of amplifiers in the performance of electrical circuits, time delays are an inevitable feature to be considered in real systems. Therefore, synchronization of neural networks with time-delays has strained an immense deal of attention in recent years [6]- [10]. From the above literature [6]- [10], the transmission of the signals from the neuron may cause few segments of networks in the characteristic delays which are named as an additive time-varying delay. Recently, the authors in [8] discussed the problem of global asymptotic stability of complex-valued neural networks with additive time-varying delays. Further, the stability analysis of neutral type neural networks with additive time-varying delay and leakage delay is studied in [9]. Therefore, it is of significant to investigate the synchronization for neural networks with additive delay which is described in [6]- [10].

On the other hand, the dynamical systems may subject to unpredictable in nature. These kinds of systems are governed by markovian chain process known as Markovian jump systems. The authors in [11] discussed the problem of stochastic synchronization of markovian jump neural networks with time-varying delay using sampled data. Recently in [12], the problem of stochastic stability analysis for Markovian jump inertial neural networks with mode-dependent time-varying delay is considered. In [13], by augmented time-dependent Lyapunov-Krasovskii functional(LKF) and zero value equality, the synchronization for Markovian coupled neural networks with mode delays via sampled-data control have been investigated. The authors in [14], studies the stochastic exponential synchronization problem for uncertain chaotic neural networks with probabilistic faults and randomly occurring time-varying parameters uncertainties. Hence, the study of Markovian jump problems for time-delay neural networks has received increasing attention.

Meanwhile, in many articles, the synchronization of neural networks has been studied by using sampled data control. The sampled data controls have been extensively applied in digital technology to save communication bandwidth. On the other hand, the sampled data control frameworks have been great deal of research in the development of communication networks, computer technology and micro electronics so on. In the sampled data control, the hybrid system grant outstanding to the coexistence of both continuous and discontinuous signals. The sampled controller has many advantages compared with continuous controller such as high reliability, maintenance with low cost, and

efficiency [15, 16]. Thus, the sampled data control method has been much attracted in the sampling information of the system. Thus, sampled-data control has annoyed extensive attention for different engineering applications [17]- [19]. In [20], the authors investigated the novel master-slave synchronization criteria of chaotic Lure systems with time delays using sampled-data control. Recently, in [21] studied the exponential sampled-data control for T–S fuzzy systems application to Chua's circuit. The main purpose of this paper, therefore, to fulfill a gap, in this article synchronization of Markovian jump neural networks for sampled data control is investigated.

According to the above discussion, the main contributions of this paper are summarized as follows:

a) Initially, the neural network model is constructed with additive time-varying delay.

b) Synchronization condition for Markovian jump neural networks with sampled data control is derived in terms of linear matrix inequalities(LMIs) which can be effectively solved by using MATLAB LMI toolbox.

c) The synchronization criteria are derived by using suitable LKF and some integral inequality technique.

d) Further, a looped functional approach is utilized to found the upper bounds of some integral terms which gave the less conservative results.

e) Results of numerical example show the effectiveness of the proposed method and the reduced conservativeness.

2 Problem Description and preliminaries

In an right-continuous Markov chain the complete probability space $(\Omega, \mathcal{F}, \mathcal{P})$ with $\{\widetilde{r}(t), t \geq 0\}$, taking values in a finite state space $\widetilde{\mathcal{S}} = \{1, 2, \ldots, \mathcal{N}\}$ with generator $\widetilde{\Gamma} = (\pi_{ij})_{\mathcal{N}\times\mathcal{N}}$ given by

$$P\{\widetilde{r}(t+\widetilde{\Delta}t) = j|\widetilde{r}(t) = i\} = \begin{cases} \pi_{ij}\widetilde{\Delta}t + o(\widetilde{\Delta}t), & i \neq j, \\ 1 + \pi_{ii}\widetilde{\Delta}t + o(\widetilde{\Delta}t), & i = j, \end{cases}$$

where $\widetilde{\Delta}t > 0$ and $\lim_{\widetilde{\Delta}t\to 0} \frac{o(\widetilde{\Delta}t)}{\widetilde{\Delta}t} = 0$, $\pi_{ij} \geq 0$ is the transition rate from i to j, if $i \neq j$ while $\pi_{ii} = -\sum_{j=1,\, j\neq i}^{\mathcal{N}} \pi_{ij}$.

The model of Markovian jump parameters with delayed neural networks is given by

$$\begin{aligned} \dot{\widetilde{x}}(t) &= -\mathcal{A}_1(\widetilde{r}(t))\widetilde{x}(t) + \mathcal{A}_2(\widetilde{r}(t))\widehat{g}(\widetilde{x}(t)) + \mathcal{A}_3(\widetilde{r}(t))\widehat{g}(\widetilde{x}(t - \widetilde{d}_1(t) - \widetilde{d}_2(t))) \\ &\quad + \mathcal{A}_4(\widetilde{r}(t)) \int_{t-\widetilde{\tau}(t)}^{t} \widehat{g}(\widetilde{x}(s))\mathrm{d}s + I(t), \end{aligned} \tag{1}$$

where $\widetilde{x}(t) = [\widetilde{x}_1(t), \widetilde{x}_2(t), \ldots, \widetilde{x}_n(t)]^T \in \mathcal{R}^n$ is the neuron state vector and $\widetilde{x}_\varpi(t)$ is the state of the ϖth neuron at time t ; $\widehat{g}(\widetilde{x}(t)) = [\widehat{g}_1(\widetilde{x}_1(t)), \widehat{g}_2(\widetilde{x}_2(t)), \ldots, \widehat{g}_n(\widetilde{x}_n(t))]^T \in \mathcal{R}^n$ denotes the neuron activation function; $\mathcal{A}_1(\widetilde{r}(t))$ is a known diagonal matrix satisfying $\mathcal{A}_1(\widetilde{r}(t)) > 0$. $\mathcal{A}_2(\widetilde{r}(t)), \mathcal{A}_3(\widetilde{r}(t))$ and $\mathcal{A}_4(\widetilde{r}(t))$ are the connection weight matrix, the delay connection weight matrix and distributively delayed connection weight matrix, respectively and $\widetilde{d}_1(t)$ and $\widetilde{d}_2(t)$ are two time-varying delays satisfying

$$0 \leq \widetilde{d}_{11} \leq \widetilde{d}_1(t) \leq \widetilde{d}_{12}, \quad 0 \leq \widetilde{d}_{21} \leq \widetilde{d}_2(t) \leq \widetilde{d}_{22}, \quad \dot{\widetilde{d}}_1(t) \leq \mu_1, \quad \dot{\widetilde{d}}_2(t) \leq \mu_2$$

where $\widetilde{d}_{12} \geq \widetilde{d}_{11}$, $\widetilde{d}_{22} \geq \widetilde{d}_{21}$ and μ_1 and μ_2 are known constants with $\widetilde{d}_{11}$ and $\widetilde{d}_{21}$ not equal to zero. Here, we denote $\widetilde{d}(t) = \widetilde{d}_1(t) + \widetilde{d}_2(t), \widetilde{d}_1 = \widetilde{d}_{11} + \widetilde{d}_{21}, \widetilde{d}_2 = \widetilde{d}_{12} + \widetilde{d}_{22}, \mu = \mu_1 + \mu_2, \bar{d}_1 = \widetilde{d}_{12} - \widetilde{d}_{11}, \bar{d}_2 = \widetilde{d}_{22} - \widetilde{d}_{21}$. $\widetilde{\tau}(t)$ is the distributed time-varying delay that satisfy $0 \leq \widetilde{\tau}(t) \leq \widetilde{\tau}$, where $\widetilde{\tau}$ is a constant.

Assumption 1: Each activation function $\widehat{g}_i(\cdot)$ is continuous and bounded, and there exist constants $\mathcal{F}_i^-$ and $\mathcal{F}_i^+$ such that

$$\mathcal{F}_i^- \leq \frac{\widehat{g}_i(\lambda_1) - \widehat{g}_i(\lambda_2)}{\lambda_1 - \lambda_2} \leq \mathcal{F}_i^+, \ \ i = 1, 2, \ldots, n$$

where $\lambda_1, \lambda_2 \in \mathbb{R}$ and $\lambda_1 \neq \lambda_2$.

The following equation represents the slave system for (1) is considered as

$$\begin{aligned} \dot{\widetilde{y}}(t) &= -\mathcal{A}_1(\widetilde{r}(t))\widetilde{y}(t) + \mathcal{A}_2(\widetilde{r}(t))\widehat{g}(\widetilde{y}(t)) + \mathcal{A}_3(\widetilde{r}(t))\widehat{g}(\widetilde{y}(t - \widetilde{d}_1(t) - \widetilde{d}_2(t))) \\ &\quad + \mathcal{A}_4(\widetilde{r}(t)) \int_{t-\widetilde{\tau}(t)}^{t} \widehat{g}(\widetilde{y}(s))\mathrm{d}s + I(t) + \hat{u}(t), \end{aligned} \tag{2}$$

where $\mathcal{A}_\nu(\widetilde{r}(t))$ for $\nu = 1, 2, 3, 4$ are matrices given in (1) and $\hat{u}(t) \in \mathcal{R}^n$ is the appropriate control input.

In order to investigate the problem of synchronization between systems (1) and (2), we define the error signal $\widetilde{e}(t) = \widetilde{y}(t) - \widetilde{x}(t)$. Therefore, the error dynamical system between (1) and (2) is given as follows:

$$\begin{aligned} \dot{\widetilde{e}}(t) &= -\mathcal{A}_1(\widetilde{r}(t))\widetilde{e}(t) + \mathcal{A}_2(\widetilde{r}(t))(\widetilde{r}(t))\widehat{f}(\widetilde{e}(t)) + \mathcal{A}_3(\widetilde{r}(t))\widehat{f}(\widetilde{e}(t - \widetilde{d}_1(t) - \widetilde{d}_2(t))) \\ &\quad + \mathcal{A}_4(\widetilde{r}(t)) \int_{t-\widetilde{\tau}(t)}^{t} \widehat{f}(\widetilde{e}(s))\mathrm{d}s + \hat{u}(t), \end{aligned} \tag{3}$$

where $\widehat{f}(\widetilde{e}(t)) = \widehat{g}(\widetilde{y}(t)) - \widehat{g}(\widetilde{x}(t))$. It can be found that the functions $\widehat{f}_i(.)$ satisfy the following condition:

$$\mathcal{F}_i^- \leq \frac{\widehat{f}_i(\alpha)}{\alpha} \leq \mathcal{F}_i^+, \ \ i = 1, 2, \ldots, n \tag{4}$$

where $\alpha \in \mathcal{R}$ and $\alpha \neq 0$.

The control input for sampled data system with state feedback control is given by

$$\hat{u}(t) = \mathcal{K}\widetilde{e}(t_k), \quad t_k \leq t < t_{k+1}, \quad k = 0, 1, 2, \cdots \tag{5}$$

where $\mathcal{K}$ represents the control gain matrix.

Then, the sampling interval satisfies the following condition

$$0 < t_{k+1} - t_k = \overline{h}_k \in [\overline{h}_l, \overline{h}_u], \quad k = 0, 1, 2, \cdots \tag{6}$$

where $\overline{h}_l$ and $\overline{h}_u$ are lower and upper bounds of the sampling periods with known positive scalars. By substituting (5) in (3), we obtain

$$\begin{aligned} \dot{\widetilde{e}}(t) &= -\mathcal{A}_1(\widetilde{r}(t))\widetilde{e}(t) + \mathcal{A}_2(\widetilde{r}(t))(\widetilde{r}(t))\widehat{f}(\widetilde{e}(t)) + \mathcal{A}_3(\widetilde{r}(t))\widehat{f}(\widetilde{e}(t - \widetilde{d}_1(t) - \widetilde{d}_2(t))) \\ &\quad + \mathcal{A}_4(\widetilde{r}(t)) \int_{t-\widetilde{\tau}(t)}^{t} \widehat{f}(\widetilde{e}(s))\mathrm{d}s + \mathcal{K}\widetilde{e}(t_k). \end{aligned} \tag{7}$$

In our convenience, the following each possible value of $\widetilde{e}(t)$ is denoted by i, $i \in \widetilde{\mathcal{S}}$. Then the system (7) can be written as

$$\begin{aligned} \dot{\widetilde{e}}(t) &= -\mathcal{A}_{1i}\widetilde{e}(t) + \mathcal{A}_{2i}\widehat{f}(\widetilde{e}(t)) + \mathcal{A}_{3i}\widehat{f}(\widetilde{e}(t - \widetilde{d}_1(t) - \widetilde{d}_2(t))) \\ &\quad + \mathcal{A}_{4i} \int_{t-\widetilde{\tau}(t)}^{t} \widehat{f}(\widetilde{e}(s))\mathrm{d}s + \mathcal{K}\widetilde{e}(t_k). \end{aligned} \tag{8}$$

Definition 1: The system (1) and (2) are said to be stochastically synchronous if error system (8) is stochastically stable with the initial condition $\widetilde{e}(t) = \psi(t)$ defined on the interval $[-\max\{\overline{d}_2, \overline{h}_u\} \quad 0]$ and $\widetilde{e}(0) \in \widetilde{\mathcal{S}}$, the following condition is satisfied:

$$\lim_{T\to\infty} \mathcal{E}\left\{\int_0^T \|\widetilde{e}(s)\|^2 \mathrm{d}s | (\psi(t), \widetilde{e}(0))\right\} < \infty. \tag{9}$$

Lemma 1 (Jensen's inequality) [22]: For any constant matrix $M \in \mathcal{R}^{n\times n}$, a scalar $\gamma > 0$, a vector function $\omega : [0, \gamma] \to \mathcal{R}^n$ such that the integrations concerned are well defined, then

$$\gamma \int_0^\gamma \omega^T(s) M \omega(s) ds \geq \Big(\int_0^\gamma \omega(s) ds\Big)^T M \Big(\int_0^\gamma \omega(s) ds\Big).$$

3 Main results

In this section, by using time-dependent Lyapunov functional approach, the stochastic synchronization of system (8) is investigated and a sufficient condition is derived to guarantee the error system to

synchronize and synthesize the stochastic sampled-data controllers in the form of (5).
In order to derive our main results, the following notations are used:

$$\mathcal{F}_1 = \text{diag}\{\mathcal{F}_1^-\mathcal{F}_1^+, \mathcal{F}_2^-\mathcal{F}_2^+, \ldots, \mathcal{F}_n^-\mathcal{F}_n^+\}, \quad \mathcal{F}_2 = \text{diag}\Big\{\frac{\mathcal{F}_1^- + F_1^+}{2}, \frac{\mathcal{F}_2^- + \mathcal{F}_2^+}{2}, \ldots, \frac{\mathcal{F}_n^- + \mathcal{F}_n^+}{2}\Big\}.$$

Theorem 1: Given a positive scalars $\overline{h}_l$, $\overline{h}_u$, γ, if there exist matrices $P_i > 0$, $\widetilde{\mathcal{Q}}_1 > 0, \widetilde{\mathcal{Q}}_2 > 0, \widetilde{\mathcal{Q}}_3 > 0, \widetilde{\mathcal{Q}}_4 > 0, \widetilde{\mathcal{Q}}_5 > 0, \widetilde{\mathcal{Q}}_6 > 0, \widetilde{\mathcal{Q}}_7 > 0, \widetilde{\mathcal{Q}}_8 > 0, \widetilde{\mathcal{Q}}_9 > 0, \widetilde{\mathcal{Q}}_{10} > 0, Z > 0$, any matrices X, Y_1, Y_2, Y_3, Y_4 satisfying the following inequalities

$$\Xi + \overline{h}_k\Pi_1 < 0, \ \begin{bmatrix} \Xi + \overline{h}_k\Phi_1 & \sqrt{\overline{h}_k}N \\ * & -Z \end{bmatrix} < 0, \tag{10}$$

where

$$\begin{aligned}
\Xi =& \text{sym}\{e_1^T P_i e_3\} + e_1^T[\sum_{j=1}^{N}\pi_{ij}P_j + \widetilde{\mathcal{Q}}_1 + \widetilde{\mathcal{Q}}_3 + \widetilde{\mathcal{Q}}_5 + \widetilde{\mathcal{Q}}_6 + \widetilde{d}_{12}^2\widetilde{\mathcal{Q}}_8 + \widetilde{d}_{22}^2\widetilde{\mathcal{Q}}_9 - \mathcal{F}_1V_{1i} - \mathcal{F}_1V_{2i} \\
&- \mathcal{F}_1V_{3i}]e_1 - e_5^T\widetilde{\mathcal{Q}}_1e_5(1-\mu_1) - e_8^T\widetilde{\mathcal{Q}}_2e_8(1-\mu_1) - e_{10}^T\widetilde{\mathcal{Q}}_3e_{10}(1-\mu_2) - e_{13}^T\widetilde{\mathcal{Q}}_4e_{13}(1-\mu_2) \\
&- e_6^T\widetilde{\mathcal{Q}}_5e_6 - e_{11}^T\widetilde{\mathcal{Q}}_6e_{11} - e_9^T\widetilde{\mathcal{Q}}_7e_9(1-\mu_1-\mu_2) - e_7^T\widetilde{\mathcal{Q}}_8e_7 - e_{12}^T\widetilde{\mathcal{Q}}_9e_{12} + e_4^T[\widetilde{\mathcal{Q}}_2 + \widetilde{\mathcal{Q}}_4 + \widetilde{\mathcal{Q}}_7 \\
&+ \tau^2\widetilde{\mathcal{Q}}_{10}]e_4 - e_{14}^T\widetilde{\mathcal{Q}}_{10}e_{14} - \overline{\alpha}^T\mathcal{Y}\overline{\alpha} + \text{sym}\{e_1^TN(e_1-e_2) + [e_1^T + \gamma e_3^T]\mathcal{G}[-e_3 - \mathcal{A}_{1i}e_1 + \mathcal{A}_{2i}e_4 \\
&+ \mathcal{A}_{3i}e_9 + \mathcal{A}_{4i}e_{14}] + e_1^T\mathcal{L}e_2 + e_3^T\gamma\mathcal{L}e_2\} + \text{sym}\{e_1^T\mathcal{F}_2V_{1i}e_4 + e_1^T\mathcal{F}_2V_{2i}e_8 + e_1^T\mathcal{F}_2V_{3i}e_{13}\} \\
&- e_4^TV_{1i}e_4 - e_8^TV_{2i}e_8 - e_{13}^TV_{3i}e_{13}, \ \Pi_1 = \text{sym}\{\overline{\varsigma}^T\mathcal{Y}\overline{\varsigma}_1\} + e_2^TXe_2 + e_3^TZe_3, \ \Phi_1 = -e_2^TXe_2 \\
&\overline{\varsigma}^T = [e_1^T \ \ e_2^T], \ \overline{\varsigma}_1^T = [e_3 \ \ 0]^T, \ \ e_\varepsilon = [0_{n\times(\varepsilon-1)n} \ \ I_n \ \ 0_{n\times(14-\varepsilon)n}], \ \varepsilon = 1, \ldots, 14.
\end{aligned}$$

then the system (1) and (2) are stochastically synchronous. Meanwhile, the desired controller gain matrix in (5) can be given by $\mathcal{K} = \mathcal{G}^{-1}\mathcal{L}$.

Proof: Constructing the following appropriate LKF:

$$\overline{\mathcal{V}}(t) = \sum_{\kappa=1}^{6}\overline{\mathcal{V}}_\kappa(t), \tag{11}$$

where

$$\begin{aligned}
\overline{\mathcal{V}}_1(t) &= \widetilde{e}^T(t)P_i\widetilde{e}(t), \\
\overline{\mathcal{V}}_2(t) &= \int_{t-\widetilde{d}_1(t)}^{t}\widetilde{e}^T(s)\widetilde{\mathcal{Q}}_1\widetilde{e}(s)\mathrm{d}s + \int_{t-\widetilde{d}_1(t)}^{t}\widehat{f}^T(\widetilde{e}(s))\widetilde{\mathcal{Q}}_2\widehat{f}(\widetilde{e}(s))\mathrm{d}s + \int_{t-\widetilde{d}_2(t)}^{t}\widetilde{e}^T(s)\widetilde{\mathcal{Q}}_3\widetilde{e}(s)\mathrm{d}s \\
&\quad + \int_{t-\widetilde{d}_2(t)}^{t}\widehat{f}^T(\widetilde{e}(s))\widetilde{\mathcal{Q}}_4\widehat{f}(\widetilde{e}(s))\mathrm{d}s + \int_{t-\widetilde{d}_1}^{t}\widetilde{e}^T(s)\widetilde{\mathcal{Q}}_5\widetilde{e}(s)\mathrm{d}s + \int_{t-\widetilde{d}_2}^{t}\widetilde{e}^T(s)\widetilde{\mathcal{Q}}_6\widetilde{e}(s)\mathrm{d}s
\end{aligned}$$

$$+\int_{t-\widetilde{d}_1(t)-\widetilde{d}_2(t)}^{t}\widehat{f}^T(\widetilde{e}(s))\widetilde{\mathcal{Q}}_7\widehat{f}(\widetilde{e}(s))\mathrm{d}s,$$

$$\overline{\mathcal{V}}_3(t)=\widetilde{d}_{12}\int_{-\widetilde{d}_{12}}^{0}\int_{t+\theta}^{t}\widetilde{e}^T(s)\widetilde{\mathcal{Q}}_8\widetilde{e}(s)\mathrm{d}s\mathrm{d}\theta+\widetilde{d}_{22}\int_{-\widetilde{d}_{22}}^{0}\int_{t+\theta}^{t}\widetilde{e}^T(s)\widetilde{\mathcal{Q}}_9\widetilde{e}(s)\mathrm{d}s\mathrm{d}\theta,$$

$$\overline{\mathcal{V}}_4(t)=\widetilde{\tau}\int_{-\widetilde{\tau}}^{0}\int_{t+\theta}^{t}\widehat{f}^T(\widetilde{e}(s))\widetilde{\mathcal{Q}}_{10}\widehat{f}(\widetilde{e}(s))\mathrm{d}s\mathrm{d}\theta,$$

$$\overline{\mathcal{V}}_5(t)=(t_{k+1}-t)\varsigma^T(t)\mathcal{Y}\varsigma(t)+(t_{k+1}-t)(t-t_k)\dot{\widetilde{e}}^T(t_k)X\widetilde{e}(t_k),$$

$$\overline{\mathcal{V}}_6(t)=(t_{k+1}-t)\int_{t_k}^{t}\dot{\widetilde{e}}^T(s)Z\dot{\widetilde{e}}(s)\mathrm{d}s,$$

and $\mathcal{Y}=\begin{bmatrix} y_1+y_1^T+y_3+y_3^T & -y_1-y_2^T-y_3-y_4^T \\ * & y_2+y_2^T+y_4+y_4^T \end{bmatrix}$, $\varsigma^T(t)=\begin{bmatrix} \widetilde{e}^T(t) & \widetilde{e}^T(t_k) \end{bmatrix}$.

By using its trajectory, the weak infinitesimal generator $\overline{\mathcal{L}}$ of the foregoing LKF is calculated, and the following equations will be obtained easily:

$$\overline{\mathcal{L}\mathcal{V}}_1(t)=2\widetilde{e}^T(t)P_i\dot{e}(t)+\widetilde{e}^T(t)\sum_{j=1}^{\mathcal{N}}\pi_{ij}P_j\widetilde{e}(t) \tag{12}$$

$$\begin{aligned}\overline{\mathcal{L}\mathcal{V}}_2(t)=&\widetilde{e}^T(t)[\widetilde{\mathcal{Q}}_1+\widetilde{\mathcal{Q}}_3+\widetilde{\mathcal{Q}}_5+\widetilde{\mathcal{Q}}_6]\widetilde{e}(t)-\widetilde{e}^T(t-\widetilde{d}_1(t))\widetilde{\mathcal{Q}}_1\widetilde{e}(t-\widetilde{d}_1(t))(1-\mu_1)\\&+\widehat{f}^T(\widetilde{e}(t))\widetilde{\mathcal{Q}}_2\widehat{f}(\widetilde{e}(t))-\widehat{f}^T(\widetilde{e}(t-\widetilde{d}_1(t)))\widetilde{\mathcal{Q}}_2\widehat{f}(\widetilde{e}(t-\widetilde{d}_1(t)))(1-\mu_1)\\&-\widetilde{e}^T(t-\widetilde{d}_2(t))\widetilde{\mathcal{Q}}_3\widetilde{e}(t-\widetilde{d}_2(t))(1-\mu_2)\\&+\widehat{f}^T(\widetilde{e}(t))\widetilde{\mathcal{Q}}_4\widehat{f}(\widetilde{e}(t))-\widehat{f}^T(\widetilde{e}(t-\widetilde{d}_2(t)))\widetilde{\mathcal{Q}}_4\widehat{f}(\widetilde{e}(t-\widetilde{d}_2(t)))(1-\mu_2)\\&-\widetilde{e}^T(t-\widetilde{d}_1)\widetilde{\mathcal{Q}}_5\widetilde{e}(t-\widetilde{d}_1)-\widetilde{e}^T(t-\widetilde{d}_2)\widetilde{\mathcal{Q}}_6\widetilde{e}(t-\widetilde{d}_2)+\widehat{f}^T(\widetilde{e}(t))\widetilde{\mathcal{Q}}_7\widehat{f}(\widetilde{e}(t))\\&-\widehat{f}^T(\widetilde{e}(t-\widetilde{d}_1(t)-\widetilde{d}_2(t)))\widetilde{\mathcal{Q}}_7\widehat{f}(\widetilde{e}(t-\widetilde{d}_1(t)-\widetilde{d}_2(t)))(1-\mu_1-\mu_2)\end{aligned} \tag{13}$$

$$\begin{aligned}\overline{\mathcal{L}\mathcal{V}}_3(t)=&\widetilde{d}_{12}^2\widetilde{e}^T(t)\widetilde{\mathcal{Q}}_8\widetilde{e}(t)+\widetilde{d}_{22}^2\widetilde{e}^T(t)\widetilde{\mathcal{Q}}_9\widetilde{e}(t)-\int_{t-\widetilde{d}_{12}}^{t}\widetilde{e}^T(s)\mathrm{d}s\widetilde{\mathcal{Q}}_8\int_{t-\widetilde{d}_{12}}^{t}\widetilde{e}(s)\mathrm{d}s\\&-\int_{t-\widetilde{d}_{22}}^{t}\widetilde{e}^T(s)\mathrm{d}s\widetilde{\mathcal{Q}}_9\int_{t-\widetilde{d}_{22}}^{t}\widetilde{e}(s)\mathrm{d}s\end{aligned} \tag{14}$$

$$\overline{\mathcal{L}\mathcal{V}}_4(t)\leq\widetilde{\tau}^2\widehat{f}^T(\widetilde{e}(t))\widetilde{\mathcal{Q}}_{10}\widehat{f}(\widetilde{e}(t))-\left(\int_{t-\widetilde{\tau}(t)}^{t}\widehat{f}^T(\widetilde{e}(s))\mathrm{d}s\right)\widetilde{\mathcal{Q}}_{10}\left(\int_{t-\widetilde{\tau}(t)}^{t}\widehat{f}(\widetilde{e}(s))\mathrm{d}s\right) \tag{15}$$

$$\begin{aligned}\overline{\mathcal{L}\mathcal{V}}_5(t)=&-\varsigma^T(t)\mathcal{Y}\varsigma(t)+2(t_{k+1}-t)\varsigma^T(t)\mathcal{Y}\dot{\varsigma}(t)-(t-t_k)\dot{\widetilde{e}}^T(t_k)X\widetilde{e}(t_k)\\&+(t_{k+1}-t)\dot{\widetilde{e}}^T(t_k)X\widetilde{e}(t_k)\end{aligned} \tag{16}$$

$$\overline{\mathcal{L}\mathcal{V}}_6(t)=(t_{k+1}-t)\dot{\widetilde{e}}^T(t)Z\dot{\widetilde{e}}(t)-\int_{t_k}^{t}\dot{\widetilde{e}}^T(s)Z\dot{\widetilde{e}}(s)\mathrm{d}s. \tag{17}$$

We consider the following zero equation,

$$0=2\widetilde{e}^T(t)N\left[\widetilde{e}(t)-\widetilde{e}(t_k)-\int_{t_k}^{t}\dot{\widetilde{e}}(s)\mathrm{d}s\right]. \tag{18}$$

From (18), we can obtain the following inequalities:

$$-2\widetilde{e}^T(t)N\int_{t_k}^{t}\dot{\widetilde{e}}(s)\mathrm{d}s \leq (t-t_k)\widetilde{e}^T(t)NZ^{-1}N^T\widetilde{e}(t)+\int_{t_k}^{t}\dot{\widetilde{e}}^T(s)Z\dot{\widetilde{e}}(s)\mathrm{d}s. \tag{19}$$

Furthermore,

$$\begin{aligned}&2\left[\widetilde{e}^T(t)+\gamma\dot{\widetilde{e}}^T(t)\right]\mathcal{G}[-\dot{\widetilde{e}}(t)-\mathcal{A}_{1i}\widetilde{e}(t)+\mathcal{A}_{2i}\widehat{f}(\widetilde{e}(t))+\mathcal{A}_{3i}\widehat{f}(\widetilde{e}(t-\widetilde{d}_1(t)-\widetilde{d}_2(t)))\\&+\mathcal{A}_{4i}\int_{t-\widetilde{\tau}(t)}^{t}\widehat{f}(\widetilde{e}(s))\mathrm{d}s+\mathcal{K}\widetilde{e}(t_k)]=0.\end{aligned} \tag{20}$$

Thus, for any approximately dimensional diagonal matrices $V_{1i}>0, V_{2i}>0$ and $V_{3i}>0$ the following inequality holds:

$$0\leq\begin{bmatrix}\widetilde{e}^T(t) & \widehat{f}^T(\widetilde{e}(t))\end{bmatrix}\begin{bmatrix}-\mathcal{F}_1V_{1i} & \mathcal{F}_2V_{1i}\\ * & -V_{1i}\end{bmatrix}\begin{bmatrix}\widetilde{e}(t)\\ \widehat{f}(\widetilde{e}(t))\end{bmatrix} \tag{21}$$

$$0\leq\begin{bmatrix}\widetilde{e}^T(t) & \widehat{f}^T(\widetilde{e}((t-\widetilde{d}_1(t)))\end{bmatrix}\begin{bmatrix}-\mathcal{F}_1V_{2i} & \mathcal{F}_2V_{2i}\\ * & -V_{2i}\end{bmatrix}\begin{bmatrix}\widetilde{e}(t)\\ \widehat{f}(\widetilde{e}(t-\widetilde{d}_1(t)))\end{bmatrix} \tag{22}$$

$$0\leq\begin{bmatrix}\widetilde{e}^T(t) & \widehat{f}^T(\widetilde{e}((t-\widetilde{d}_2(t)))\end{bmatrix}\begin{bmatrix}-\mathcal{F}_1V_{3i} & \mathcal{F}_2V_{3i}\\ * & -V_{3i}\end{bmatrix}\begin{bmatrix}\widetilde{e}(t)\\ \widehat{f}(\widetilde{e}(t-\widetilde{d}_2(t)))\end{bmatrix} \tag{23}$$

From (12)–(17) and adding (18)–(23) and $\overline{h}_k\in[\overline{h}_l,\overline{h}_u]$, the following inequality is obtained:

$$\overline{\mathcal{LV}}(t)\leq\varrho^T(t)\left(\frac{t_{k+1}-t}{\overline{h}_k}\left(\Xi+\overline{h}_k\Pi_1\right)+\frac{t-t_k}{\overline{h}_k}\left(\Xi+\overline{h}_k\Phi_1+\overline{h}_kNZ^{-1}N^T\right)\right)\varrho(t). \tag{24}$$

where

$$\begin{aligned}\varrho^T(t) \;=\; &\Big[\widetilde{e}^T(t)\ \widetilde{e}^T(t_k)\ \dot{\widetilde{e}}^T(t)\ \widehat{f}^T(\widetilde{e}(t))\ \widetilde{e}^T(t-\widetilde{d}_1(t))\ \widetilde{e}^T(t-\widetilde{d}_1)\ \int_{t-\widetilde{d}_{12}}^{t}\widetilde{e}^T(s)\mathrm{d}s\\&\widehat{f}^T(\widetilde{e}(t-\widetilde{d}_1(t))\ \widehat{f}^T(\widetilde{e}(t-\widetilde{d}_1(t)-\widetilde{d}_2(t)))\ \widetilde{e}^T(t-\widetilde{d}_2(t))\ \widetilde{e}^T(t-\widetilde{d}_2)\\&\int_{t-\widetilde{d}_{22}}^{t}\widetilde{e}^T(s)\mathrm{d}s\ \widehat{f}^T(\widetilde{e}(t-\widetilde{d}_2(t))\ \int_{t-\tau(t)}^{t}\widehat{f}^T(\widetilde{e}(s))\mathrm{d}s\Big].\end{aligned}$$

Hence, (10) guarantees that

$$\overline{\mathcal{LV}}(t)\leq-\gamma\|\widetilde{e}(t)\|^2 \tag{25}$$

for some $\gamma>0$. Now, using Dynkin's formula, we have that, for all $T\geq0$

$$\mathcal{E}\{\overline{\mathcal{V}}(t)\}-\mathcal{E}\{\overline{\mathcal{V}}(0)\}\leq-\gamma\mathcal{E}\left\{\int_0^T\|\widetilde{e}(s)\|^2\mathrm{d}s\right\}. \tag{26}$$

Hence

$$\mathcal{E}\left\{\int_0^T \|\widetilde{e}(s)\|^2 \mathrm{d}s\right\} \leq \gamma^{-1}\mathcal{E}\{\overline{\mathcal{V}}(0)\}. \tag{27}$$

which implies that (9) holds. Therefore, from Definition 1, we have that master system (1) and slave system (2) are stochastically synchronous. This completes the proof.

Remark 1: It is appropriate to note that Theorem 1, provides a new synchronization criterion for the master and slave system. Our main intention in Theorem 1 is to study the Lyapunov stability theory by involving looped functional technique. Meanwhile, the proposed conditions in this Theorem 1 are expressed in the form of LMIs. Further, the computation of the terms in the LMIs can be simplified by reducing the parameters involved in the LKFs. Thus, the criteria taken in the LKF which has not been considered in the previous works [11, 13, 15, 23–26], which leaves us much room to investigate the problem of synchronization for neural networks with additive time-varying delay by looped-functional technique.

Remark 2: It is note that, the LKF constructed in the proof of Theorem 1 is more different with those in [13, 15]. Further, in this paper the augmented looped functional $\overline{\mathcal{V}}_5(t)$ and $\overline{\mathcal{V}}_6(t)$ have been introduced in the lyapunov functional, which consider the information of states $\zeta^T(t)$. Due to fewer constraints on the lyapunov functional the looped functional method proposed in this article can give less computational burden. Thus, the LKF taken in this paper represent a more general form.

Remark 3: In the additive time-varying delay, the information transmitted between the sensors, actuators and controllers trade information over the system. The planned delay has a physically powerful application background in networked control and long-range control. Such delays persuade through an assortment of communication modes are usually time-varying and display dissimilar substantial properties. In the modern trends, it can be professed that synchronization problem of various neural networks has been paying attention in [11, 13, 15, 23, 24]. Therefore, the representation of neural networks with two additive time varying delay components is proposed due to practical application background. On the other hand, in the existing literature [11, 13, 15, 23, 24] synchronization methods does not fully consider the information of two additive time-varying delay components. Based on the above discussion, it should be pointed out that, the additive delay designed in Theorem 1 is to investigate a synchronization for Markovian jump neural networks. Thus, the synchronization problem for Markovian jump neural networks with additive time delays has not been fully discussed, this motivates our current research.

Specifically, when there is no distributed delay and if we choose single time-delay in (1) (i.e. $\widetilde{d}_1(t)$ only, $\widetilde{d}_2(t) = 0$) neural network (1) and (2) reduce to the following systems, respectively

$$\dot{\widetilde{x}}(t) = -\mathcal{A}_1(\widetilde{r}(t))\widetilde{x}(t) + \mathcal{A}_2(\widetilde{r}(t))\widehat{g}(\widetilde{x}(t)) + \mathcal{A}_3(\widetilde{r}(t))\widehat{g}(\widetilde{x}(t-\widetilde{d}_1(t)) + I(t) \tag{28}$$

and

$$\dot{\widetilde{y}}(t) = -\mathcal{A}_1(\widetilde{r}(t))\widetilde{y}(t) + \mathcal{A}_2(\widetilde{r}(t))\widehat{g}(\widetilde{y}(t)) + \mathcal{A}_3(\widetilde{r}(t))\widehat{g}(\widetilde{y}(t-\widetilde{d}_1(t)) + I(t) + \hat{u}(t) \quad (29)$$

Correspondingly, the error system (7) reduces to

$$\dot{\widetilde{e}}(t) = -\mathcal{A}_1(\widetilde{r}(t))\widetilde{e}(t) + \mathcal{A}_2(\widetilde{r}(t))(\widetilde{r}(t))\widehat{f}(\widetilde{e}(t)) + \mathcal{A}_3(\widetilde{r}(t))\widehat{f}(\widetilde{e}(t-\widetilde{d}_1(t))) + \hat{u}(t). \quad (30)$$

where $\widetilde{d}_1(t)$ satisfies

$$0 \leq \widetilde{d}_{11} \leq \widetilde{d}_1(t) \leq \widetilde{d}_{12}, \quad \dot{\widetilde{d}}_1(t) \leq \mu_1,$$

Therefore, system (30) is the particular case of system (8). Consider the following Lyapunov functional for the error system (30)

$$\overline{\mathcal{V}}_2(t) = \int_{t-\widetilde{d}_1(t)}^{t} \widetilde{e}^T(s)\widetilde{\mathcal{Q}}_1\widetilde{e}(s)\mathrm{d}s + \int_{t-\widetilde{d}_1(t)}^{t} \widehat{f}^T(\widetilde{e}(s))\widetilde{\mathcal{Q}}_2\widehat{f}(\widetilde{e}(s))\mathrm{d}s + \int_{t-\widetilde{d}_1}^{t} \widetilde{e}^T(s)\widetilde{\mathcal{Q}}_5\widetilde{e}(s)\mathrm{d}s,$$
$$\overline{\mathcal{V}}_3(t) = \widetilde{d}_{12}\int_{-\widetilde{d}_{12}}^{0}\int_{t+\theta}^{t} \widetilde{e}^T(s)\widetilde{\mathcal{Q}}_8\widetilde{e}(s)\mathrm{d}s\mathrm{d}\theta$$

where $\overline{\mathcal{V}}_4(t) = 0$, $\overline{\mathcal{V}}_1(t), \overline{\mathcal{V}}_5(t), \overline{\mathcal{V}}_6(t)$ follow the same definitions as those in (11). By using the similar method employed in the proof of Theorem 1, we can easily obtain the following result.

Theorem 2: Given a positive scalars $\overline{h}_l$, $\overline{h}_u$, γ, if there exist matrices $P_i > 0$, $\widetilde{\mathcal{Q}}_1 > 0, \widetilde{\mathcal{Q}}_2 > 0, \widetilde{\mathcal{Q}}_5 > 0, \widetilde{\mathcal{Q}}_8 > 0, Z > 0$, any matrices X, Y_1, Y_2, Y_3, Y_4 satisfying the following inequalities

$$\Xi + \overline{h}_k\Pi_1 < 0, \begin{bmatrix} \Xi + \overline{h}_k\Phi_1 & \sqrt{\overline{h}_k}N \\ * & -Z \end{bmatrix} < 0, \quad (31)$$

where

$$\begin{aligned}
\Xi =& \mathrm{sym}\{e_1^T P_i e_3\} + e_1^T[\sum_{j=1}^{\mathcal{N}}\pi_{ij}P_j + \widetilde{\mathcal{Q}}_1 + \widetilde{\mathcal{Q}}_5 + \widetilde{d}_{12}^2\widetilde{\mathcal{Q}}_8 - \mathcal{F}_1V_{1i} - \mathcal{F}_1V_{2i}]e_1 - e_5^T\widetilde{\mathcal{Q}}_1e_5(1-\mu_1) \\
& - e_8^T\widetilde{\mathcal{Q}}_2e_8(1-\mu_1) - e_6^T\widetilde{\mathcal{Q}}_5e_6 - e_7^T\widetilde{\mathcal{Q}}_8e_7 - \overline{\alpha}^T\mathcal{Y}\overline{\alpha} + \mathrm{sym}\{e_1^TN(e_1-e_2) \\
& + [e_1^T + \gamma e_3^T]\mathcal{G}[-e_3 - \mathcal{A}_{1i}e_1 + \mathcal{A}_{2i}e_4 + \mathcal{A}_{3i}e_8 + e_1^T\mathcal{L}e_2 + e_3^T\gamma\mathcal{L}e_2]\} \\
& + \mathrm{sym}\{e_1^T\mathcal{F}_2V_{1i}e_4 + e_1^T\mathcal{F}_2V_{2i}e_8\} - e_4^TV_{1i}e_4 - e_8^TV_{2i}e_8, \\
\Pi_1 =& \mathrm{sym}\{\overline{\varsigma}^T\mathcal{Y}\overline{\varsigma}_1\} + e_2^TXe_2 + e_3^TZe_3,\ \Phi_1 = -e_2^TXe_2,\ \overline{\varsigma}^T = [e_1^T\ \ e_2^T],\ \overline{\varsigma}_1^T = [e_3\ \ 0]^T, \\
e_\varepsilon =& [0_{n\times(\varepsilon-1)n}\ \ I_n\ \ 0_{n\times(8-\varepsilon)n}],\ \varepsilon = 1,\ldots,8.
\end{aligned}$$

then master system (28) and slave system (29) are stochastically synchronous. Moreover, the desired controller gain matrix in (5) can be given by $\mathcal{K} = \mathcal{G}^{-1}\mathcal{L}$.

4 Illustrative Examples

In this section, numerical examples are given to demonstrate the effectiveness and applicability of the considered system.

Example 1: Consider the following master system and slave system of Markovian jump delayed neural networks as follows:

$$\begin{aligned}\dot{\widetilde{x}}(t) &= -\mathcal{A}_{1i}\widetilde{x}(t) + \mathcal{A}_{2i}\widehat{g}(\widetilde{x}(t)) + \mathcal{A}_{3i}\widehat{g}(\widetilde{x}(t-\widetilde{d}_1(t)-\widetilde{d}_2(t))) \\ &\quad +\mathcal{A}_{4i}\int_{t-\widetilde{\tau}(t)}^{t}\widehat{g}(\widetilde{x}(s))\mathrm{d}s + I(t), \end{aligned} \tag{32}$$

$$\begin{aligned}\dot{\widetilde{y}}(t) &= -\mathcal{A}_{1i}\widetilde{y}(t) + \mathcal{A}_{2i}\widehat{g}(\widetilde{y}(t)) + \mathcal{A}_{3i}\widehat{g}(\widetilde{y}(t-\widetilde{d}_1(t)-\widetilde{d}_2(t))) \\ &\quad +\mathcal{A}_{4i}\int_{t-\widetilde{\tau}(t)}^{t}\widehat{g}(\widetilde{y}(s))\mathrm{d}s + I(t) + \hat{u}(t) \quad (i=1,\,2) \end{aligned} \tag{33}$$

where

$$\mathcal{A}_{11} = \begin{bmatrix} 2.01 & 0 \\ 0 & 1.28 \end{bmatrix}, \quad \mathcal{A}_{12} = \begin{bmatrix} 4 & 0 \\ 0 & 3.33 \end{bmatrix}, \quad \mathcal{A}_{21} = \begin{bmatrix} 1 & -0.17 \\ -2.8 & 2.3 \end{bmatrix},$$
$$\mathcal{A}_{22} = \begin{bmatrix} 1.17 & -0.26 \\ -3.4 & 2.5 \end{bmatrix}, \ \mathcal{A}_{31} = \begin{bmatrix} -1.36 & -0.26 \\ -0.2 & -2.24 \end{bmatrix}, \ \mathcal{A}_{32} = \begin{bmatrix} -1.9 & -0.1 \\ -0.9 & -2.02 \end{bmatrix},$$
$$\mathcal{A}_{41} = \begin{bmatrix} 0.2 & 1.32 \\ 2.28 & -0.18 \end{bmatrix}, \quad \mathcal{A}_{42} = \begin{bmatrix} 0.8 & 1.1 \\ 2.22 & -0.25 \end{bmatrix}.$$

The nonlinear activation functions are taken as

$$\widehat{g}_1(\kappa) = \widehat{g}_2(\kappa) = \frac{|\kappa+1| - |\kappa-1|}{2}$$

with $\mathcal{F}_1^- = \mathcal{F}_2^- = 0$ and $\mathcal{F}_1^+ = \mathcal{F}_2^+ = 1$. Thus,

$$\mathcal{F}_1 = \begin{bmatrix} 0 & 0 \\ 0 & 0 \end{bmatrix}, \quad \mathcal{F}_2 = \begin{bmatrix} 0.5 & 0 \\ 0 & 0.5 \end{bmatrix}.$$

The transition probability matrix is given by

$$\widetilde{\Gamma} = \begin{bmatrix} -5 & 5 \\ 5 & -5 \end{bmatrix}.$$

Assume $I(t) = 0$, $\gamma = 0.03$ and discrete delay as $\widetilde{d}_1(t) = 4e^t/(10e^t+10)$, $\widetilde{d}_2(t) = 6e^t/(10e^t+10)$ and distributed delay $\widetilde{\tau}(t) = 1.2|\cos(t)|$. Hence, a straightforward calculation gives $\widetilde{d}_{11} = 0.2$, $\widetilde{d}_{12} = 0.4$, $\mu_1 = 0.1$, $\widetilde{d}_{21} = 0.3$, $\widetilde{d}_{22} = 0.6, \mu_2 = 0.15$ and $\widetilde{\tau} = 1.2$. By using Theorem 1

and MATLAB LMI toolbox, the feasible solution is obtained for the given values $\widetilde{d}_{11} = 0.2$, $\widetilde{d}_{12} = 0.4$, $\widetilde{d}_{21} = 0.3$, $\widetilde{d}_{22} = 0.6$ with the initial conditions as $\widetilde{x}(t) = \{[-0.2\ \ -0.2]^T, [0.2\ 0.2]^T\}$ and $\widetilde{y}(t) = \{[0.4\ 0.4]^T, [-0.2\ \ -0.2]^T\}$, $t \in [-1\ 0]$ respectively. In addition, Figure 1 and Figure 2 represent the chaotic behavior of the system (1) without control input. The gain matrix for Theorem 1 is shown in Table 1 by using LMI toolbox. Figure 3, shows the synchronization of master and slave

Table 1: The Control gain Matrix for Example 1

Allowable values of $\mu_1,\ \mu_2$ and sampling periods	gain matrix
By Theorem 1, $\mu_1 = 0.1,\ \mu_2 = 0.15,\ \overline{h}_l = 0.1,\ \overline{h}_u = 0.5$	$\mathcal{K} = \begin{bmatrix} -43.3850 & 5.8849 \\ 22.9808 & -37.3222 \end{bmatrix}$

system with the action of the gain matrix $\mathcal{K}$. The state responses of the error system (8) without and with $\hat{u}(t)$ are displayed in Figures 3 and 4, respectively. controller $\hat{u}(t_k)$ (5) are demonstrated in Figure 5.

Example 2: Consider the system (28) and (29) of delayed neural networks with the following parameters:

$$\mathcal{A}_{11} = \begin{bmatrix} 1 & 0 \\ 0 & 0.9 \end{bmatrix}, \mathcal{A}_{21} = \begin{bmatrix} 0.9 + \frac{\pi}{4} & 19 \\ 0.11 & 0.9 + \frac{\pi}{4} \end{bmatrix}, \mathcal{A}_{31} = \begin{bmatrix} -1.2\sqrt{2}\frac{\pi}{4} & 0.3 \\ 0.2 & -1.2\sqrt{2}\frac{\pi}{4} \end{bmatrix},$$
$$\mathcal{A}_{12} = \begin{bmatrix} 1 & 0 \\ 0 & 1 \end{bmatrix}, \mathcal{A}_{22} = \begin{bmatrix} 1 + \frac{\pi}{4} & 19 \\ 0.09 & 1 + \frac{\pi}{4} \end{bmatrix}, \mathcal{A}_{32} = \begin{bmatrix} -1.3\sqrt{2}\frac{\pi}{4} & 0.1 \\ 0.1 & -1.3\sqrt{2}\frac{\pi}{4} \end{bmatrix}.$$

The nonlinear activation functions are taken as

$$\widehat{g}_1(\kappa) = \widehat{g}_2(\kappa) = \frac{|\kappa + 1| - |\kappa - 1|}{2}$$

with $\mathcal{F}_1^- = \mathcal{F}_2^- = 0$ and $\mathcal{F}_1^+ = \mathcal{F}_2^+ = 1$. Thus,

$$\mathcal{F}_1 = \begin{bmatrix} 0 & 0 \\ 0 & 0 \end{bmatrix}, \quad \mathcal{F}_2 = \begin{bmatrix} 0.5 & 0 \\ 0 & 0.5 \end{bmatrix}.$$

The transition probability matrix is given by

$$\widetilde{\Gamma} = \begin{bmatrix} -0.5 & 0.5 \\ 0.8 & -0.8 \end{bmatrix}.$$

Assume $I(t) = 0$, $\gamma = 0.3$ and discrete delay as $\widetilde{d}_1(t) = e^t/(e^t + 1)$. By setting, the values $\widetilde{d}_{11} = 0.5$, $\widetilde{d}_{12} = 1$, $\mu_1 = 0.25$ and using Theorem 2 with MATLAB LMI toolbox the feasible solutions are obtained. The initial conditions of system (28) and (29) are given by $\widetilde{x}(t) =$

$\{[-0.25\ \ -0.25]^T, [-0.35\ \ -0.35]^T\}$ and $\widetilde{y}(t) = \{[0.27\ 0.27]^T, [0.30\ 0.30]^T\}$, $t \in [-1\ 0]$ respectively. In addition, the controller gain matrix $\mathcal{K}$ is given by, $\mathcal{K} = \begin{bmatrix} -210.1309 & -24.4214 \\ -52.4999 & -50.1488 \end{bmatrix}$. Meanwhile, the maximum sampling interval $\overline{h}_k$ is calculated for $\gamma = 0.3$ are compared to that of [11] and [27] and given in Table 2. Furthermore, it is worth pointing out that Theorem 2 yields less conservative results than the existing literature. Figure 6 and 7, shows the chaotic behavior of the given system without control input. In Figure 8, the synchronization behavior of the master and slave system with the action of the gain matrix is drawn. Meanwhile, the state responses of the error system (30) with controller $\hat{u}(t_k)$ are predicted in Figure 8 and 9.

Remark 4: In [11], the synchronization performance of neural networks with time-varying delay and sampled data control has been investigated by linear matrix inequality. By constructing an augmented Lyapunov functional and combining, a new integral inequality technique, sufficient synchronization conditions are established in [27]. In Table 2, the obtained results for maximum sampling interval $\overline{h}_k$ using Theorem 2 are compared with those obtained by various approached proposed in [11, 27]. It is clear from Table 2, one can get that in [11] and [27], the maximum sampling intervals are 0.2859 and 0.7757, so as to realize the stochastic synchronization of the objective systems. By analyzing with the results obtained in [11], the upper bound of our sampling interval $\overline{h}_k$ can reach the maximum of 0.9258 under the declaration of establishing the same parameters of the desired system. It can be witnessed from Table 2 that the values of sampling interval $\overline{h}_k$ are significantly larger than those of [11, 27], which clearly indicates that the proposed synchronization criterion in Theorem 2 lead to less conservative results than those of [11, 27]. Hence, the superiority of our results can be fully shown in Example 2.

Table 2: Maximum sampling interval $\overline{h}_k$ for different methods with $\gamma = 0.3$

Methods	Theorem 1/2 in [11]	Theorem 2 in [27]	Theorem 2
$\overline{h}_k$	0.1610/0.2859	0.7757	0.9258

Example 3: In the modern days, Security plays a vital role in communication and storage of images, and encryption is one of the ways to ensure security. Image encryption has fast growth in digital image processing and extensive propagation of digital multimedia data over the Internet has made us to defend this imperative information against illegal copying and distribution. According to the properties of random similarity and parameter sensitivity, a neural network has been used in Image encryption. For example, in [28] constructed the image encryption algorithm based on memristor chaotic system. Inspired by the above application, in this example an image encryption is considered.

In Example 1, the delayed neural networks has been attracted the great chaotic behavior, and it can be applied to image encryption. Further, the experimental analysis of the proposed image encryption has been done in this example. The dimension of the image is denoted as m row n column and 3 number of pixels. Moreover, the plain image with the size 256×256 is shown in Figure 10. The encryption procedure is given as follows

Encryption Procedure for plain image

$p =: 1; q =: 1; r =: 1;$

for p to m do

for q to n do

$\check{\mathsf{z}}_1(p,q) := (10^8 \times (\check{\mathsf{z}}_1(k) - [\check{\mathsf{z}}_1(k)])) \mod 256$

$\check{\mathsf{z}}_2(p,q) := (10^8 \times (\check{\mathsf{z}}_2(k) - [\check{\mathsf{z}}_2(k)])) \mod 256$

$\check{\mathsf{z}}_3(p,q) := (10^8 \times (\check{\mathsf{z}}_3(k) - [\check{\mathsf{z}}_3(k)])) \mod 256$

$\breve{R}(p,q) := \breve{R}(p,q)\, \mathcal{XOR}\, \check{\mathsf{z}}_1(p,q);$

$\breve{G}(p,q) := \breve{G}(p,q)\, \mathcal{XOR}\, \check{\mathsf{z}}_2(p,q);$

$\breve{B}(p,q) := \breve{B}(p,q)\, \mathcal{XOR}\, \check{\mathsf{z}}_3(p,q);$

end for

end for

1) The four chaotic sequences are generated in master system (32) and slave system (34) in Example 1 is denoted by $x_1(t), x_2(t), y_1(t), y_2(t)$. Colors of the plain image P can be represented with three color components that is red, green and blue, then it separated into three pixel sequences: $\breve{R}(p,q), \breve{G}(p,q)$ and $\breve{B}(p,q)$, where $p = 1, 2, \ldots, m, q = 1, 2, \ldots, n$.
2) The chaotic behavior $x_1(t)$ is arranged in ascending order to obtain the index term pdx of the sorted $x_1(t)$. To apply permutation operation into the considered image, the following procedure is described:

$$\hat{R}(k) := \breve{R}(pdx((p-1) \times n + q)),$$
$$\hat{G}(k) := \breve{G}(pdx((p-1) \times n + q)),$$
$$\hat{B}(k) := \breve{B}(pdx((p-1) \times n + q)),$$
$$\breve{R}(p;q) := \hat{R}(k),\ \breve{G}(p;q) := \hat{G}(k),\ \breve{B}(p;q) := \hat{B}(k).$$

where $k = 1, 2, \ldots, mn$, $p = 1, 2, \ldots, n$, $q = 1, 2, \ldots, m$; $\hat{R}, \hat{G}, \hat{B}$ are sequences with the size of $m \times n$.

3) The chaotic behavior $x_2(t), y_1(t), y_2(t)$ are transformed into $m \times n$ matrices $\check{z}_1, \check{z}_2, \check{z}_3$ as follows: $\check{z}_1(p;q) := X_2,\ \check{z}_2(p;q) := Y_1,\ \check{z}_3(p;q) := Y_2$.
4)The Matrices $\check{z}_1, \check{z}_2, \check{z}_3$ is used to cipher the prescribed images $\breve{R}(p,q), \breve{G}(p,q)$ and $\breve{R}(p,q)$ according to encryption procedure, respectively. After changing the $\breve{R}(p,q), \breve{G}(p,q)$ and $\breve{B}(p,q)$ components the cipher image $[\check{z}_p(k)]$ is obtained which is equivalent to $floor(\check{z}_p(k))$.

Hence the encryption process is concluded and the ciphered image is obtained. The simulations about color image encryption have provided in Figures 10 and 11, respectively. It should be noted that, the histograms of the test images and their corresponding cipher images are obtained by our improved encryption algorithm shown in Figure 12. The variances of histograms of the tested plain images (size of 256×256) and their corresponding cipher images are listed in Table 3. In Table 3, it can be seen that the plain image has strong correlations between neighborhood pixels, while correlations of the encrypted image are weak.

Table 3: Correlation coefficients of adjacent pixel in the original image and in the encrypted image

	Plain image	Encrypted image
horizontal direction	0.9917	0.5508
vertical direction	0.9920	0.5013
diagonal direction	0.9869	0.5006

5 Conclusion

In this article, the synchronization problem of Markovian jump neural networks with additive time delay has been investigated via sampled-data control. By defining appropriate LKF and using a novel looped functional approach, a new synchronization criteria have been derived in terms of LMIs. The

conditions established in Theorem 1 reduce less computational burden and guarantee the synchronization of Master-Slave systems. Further, the sampled-data controller gain matrix are solved by the LMIs, under the allowable maximum sampling period. Finally, the advantages of the looped functional method and synchronization involved in image encryption criteria have been demonstrated via numerical examples.

References

[1] L.M. Pecora, T.L Carroll, Synchronization in chaotic systems, Physics Review Letter, 64 (1990) 821–824.

[2] J.J. Huang, C.D Li, T.W. Huang, X. He, Finite-time lag synchronization of delayed neural networks, Neurocomputing, 139 (2014) 145-149 .

[3] G. Mahmoud, E. Mahmoud, Lag synchronization of hyper-chaotic complex nonlinear systems, Nonlinear Dynamics, 67 (2012) 1613–1622.

[4] Z. Qian, X. Wang, S. Zu, A preamble patten identification based synchronization system for UWB-based wireless networks, Journal of Networks, 7 (2012) 660–666.

[5] X. Wu, C. Bai, H. Kan, A new color image cryptosystem via hyperchaos synchronization, Communication in Nonlinear Science and Numerical Simulation, 19 (2014) 1884–1897.

[6] H. Chen, Improved stability criteria for neural networks with two additive time-varying delay Components, Circuits Systems and Signal Processing, 32 (2013) 1977–1990.

[7] G. Nagamani, T. Radhika, Q. Zhu, An improved result on dissipativity and passivity analysis of Markovian jump stochastic neural networks with two delay components, IEEE Transactions on neural networks and Learning systems, 28 (2016) 3018–3031.

[8] K. Subramanian, P. Muthukumar, Global asymptotic stability of complex-valued neural networks with additive time-varying delays, Cognitive Neurodynamics, 11 (2017) 293–306.

[9] L. Ding, Y. He, Y. Liao, M. Wu, New result for generalized neural networks with additive time-varying delays using free-matrix-based integral inequality method, Neurocomputing, 238 (2017) 205–211.

[10] R. Samidurai, S. Rajavel, R. Sriraman, J. Cao, A. Alsaedi, F.E. Alsaadi, Novel results on stability analysis of neutral-type neural networks with additive time-varying delay components and leakage delay, International Journal of Control, Automation and Systems, 15 (2017) 1–13.

[11] Z.G. Wu, P. Shi, H. Su, J. Chu, Stochastic synchronization of Markovian jump neural networks With time-varying delay using sampled data, IEEE Transactions On Cybernetics, 43 (2013) 1796–1806.

[12] R. Krishnasamy, R.K. George, Stochastic stability of mode dependent Markovian jump inertial neural networks, The Journal of Analysis, 27 (2019) 179–196.

[13] D. Zeng, K. T. Wu, R. Zhang, S. Zhong, K. Shi, Improved results on sampled-data synchronization of Markovian coupled neural networks with mode delays, Neurocomputing, 275 (2018) 2845–2854.

[14] K. Shi, J. Wang, S. Zhong, X. Zhang, Y. Liu, J. Cheng, New reliable nonuniform sampling control for uncertain chaotic neural networks under Markov switching topologies, Applied Mathematics and Computation, 347 (2019) 169–193.

[15] R. Zhang, D. Zeng, S. Zhong, Novel master-slave synchronization criteria of chaotic Lure systems with time delays using sampled-data control, Journal of Franklin Institute, 354 (2017) 4930–4954.

[16] A. Seuret, C. Briat, Stability analysis of uncertain sampled-data systems with incremental delay using looped-functionals, Automatica, 55 (2015) 274–278.

[17] T.H. Lee, Ju. H. Park, Improved criteria for sampled-data synchronization of chaotic Lure systems using two new approaches, Nonlinear Analysis and Hybrid Systems, 24 (2017) 132-145.

[18] T.H. Lee, J.H. Park, Stability analysis of sampled-data systems via free-matrix-based time-dependent discontinuous Lyapunov approach, IEEE Transactions on Automatic Control, 62 (2017) 3653-3657.

[19] C. Ge, B. Wang, X. Wei, Y. Liu, Exponential synchronization of a class of neural networks with sampled-data control, Applied Mathematics and Computation, 315 (2017) 150-161.

[20] R. Zhang, D. Zeng, S. Zhong, Novel master-slave synchronization criteria of chaotic Lure systems with time delays using sampled-data control, Journal of the Franklin Institute, doi: 10.1016/j.jfranklin.2017.05.008.

[21] N. Gunasekaran, R. Saravanakumar, M. Syed Ali, Quanxin Zhu, Exponential sampled-data control for T-S fuzzy systems: application to Chua's circuit, International Journal of Systems Science, 50 (2019) 2979–2992.

[22] K. Gu, V. Kharitonov, J. Chen, Stability of Time-delay Systems, Birkhauser, MA, (2003).

[23] T. Fang, S. Tiao, D. Fu, L. Su, Passivity-based synchronization for Markov switched neural networks with time delays and the inertial term, Applied Mathematics and Computation 394 (2021) 125786.

[24] R. Zhang, D. Zeng, J. H. Park, Y. Liu, S. Zhong, Quantized sampled-data control for synchronization of inertial neural networks with heterogeneous time-varying delays, IEEE Transactions on Neural Networks and Learning Systems, 99 (2018) 1-11.

[25] X. Song, R. Zhang, M. Wang, Nonfragile dissipative synchronization of reaction-diffusion complex dynamical networks with coupling delays. International Journal of Control, Automation and systems, 19 (2021) 1252-1263.

[26] W. Li, X. Gao, R. Li, Stability and synchronization control of inertial neural networks with mixed delays, Applied Mathematics and Computation, 367 (2020) 124779.

[27] H. Shen, S. Jiao, J. Cao, T. Huang, An Improved Result on Sampled-Data Synchronization of Markov Jump Delayed Neural Networks, IEEE Transactions On Systems, Man and Cybernetics: Systems, doi: 10.1109/TSMC.2019.2931533.

[28] B. Wang, F.C. Zou, J. Cheng, A memristor-based chaotic system and its application in image encryption, Optik, 154 (2018) 538–544.

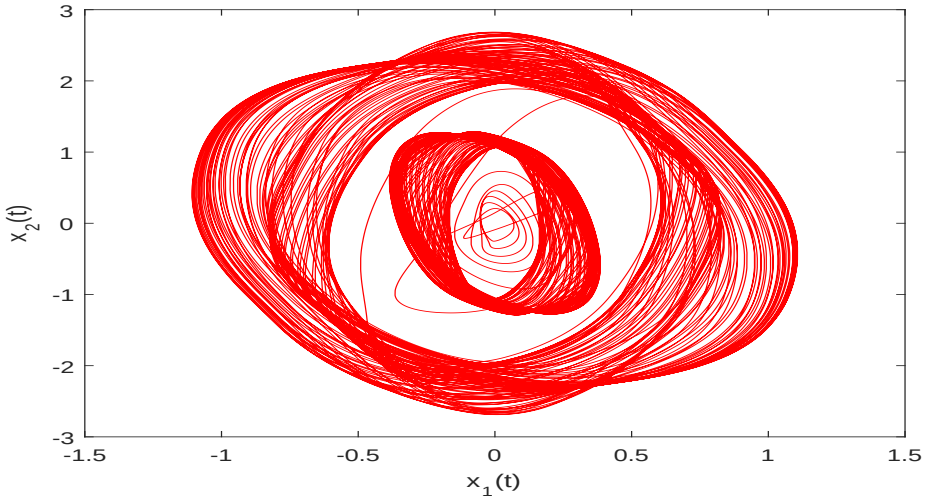

Figure 1: Chaotic behavior of master system (1) with $u(t) = 0$.

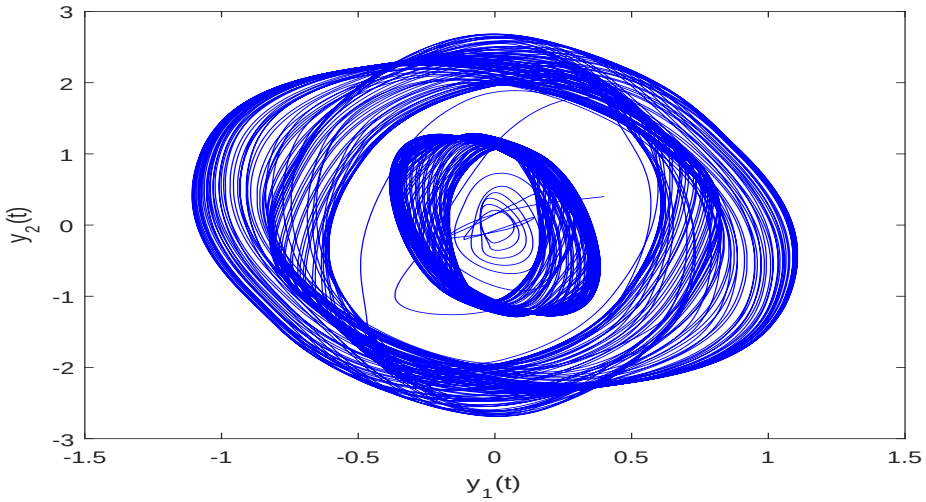

Figure 2: Chaotic behavior of slave system (2) with $u(t) = 0$.

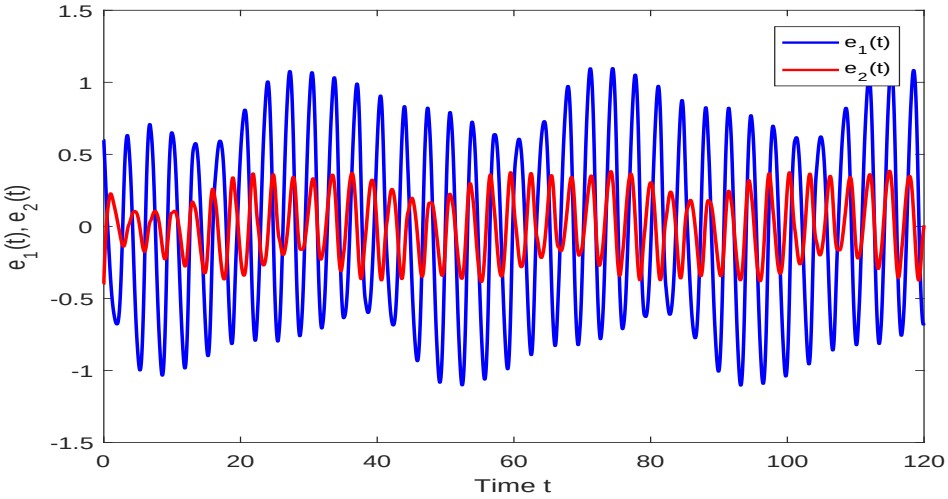

Figure 3: State responses of error system (8) with u(t)=0.

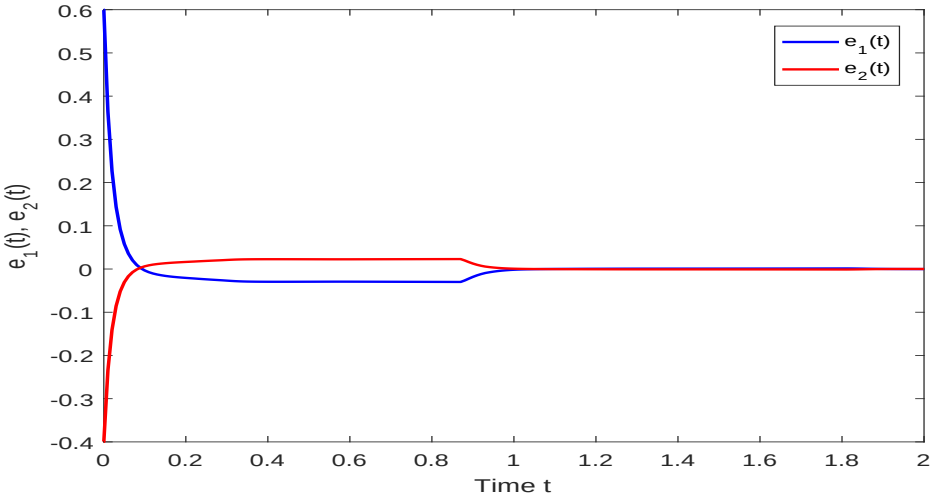

Figure 4: State responses of error system (8).

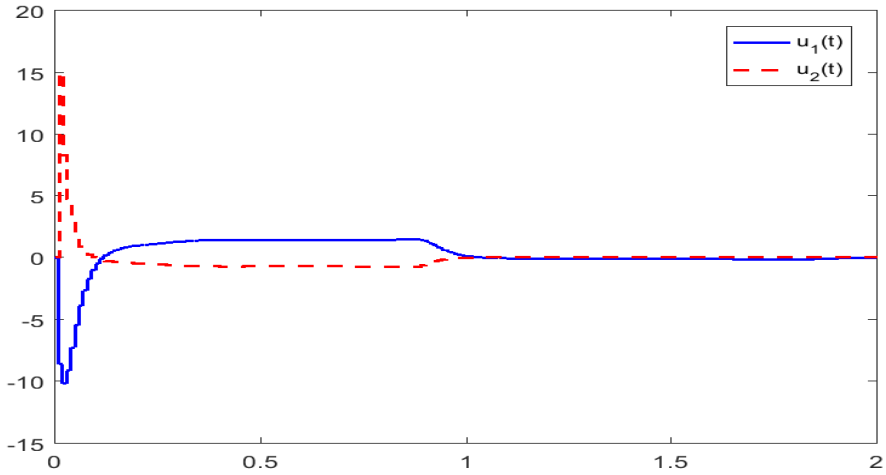

Figure 5: Control input $u(t_k)$.

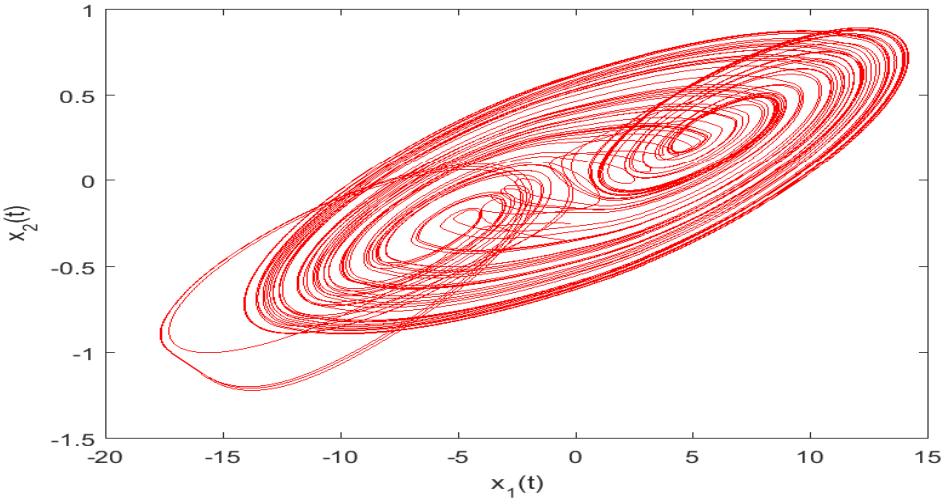

Figure 6: Chaotic behavior of master system (28) with $u(t) = 0$.

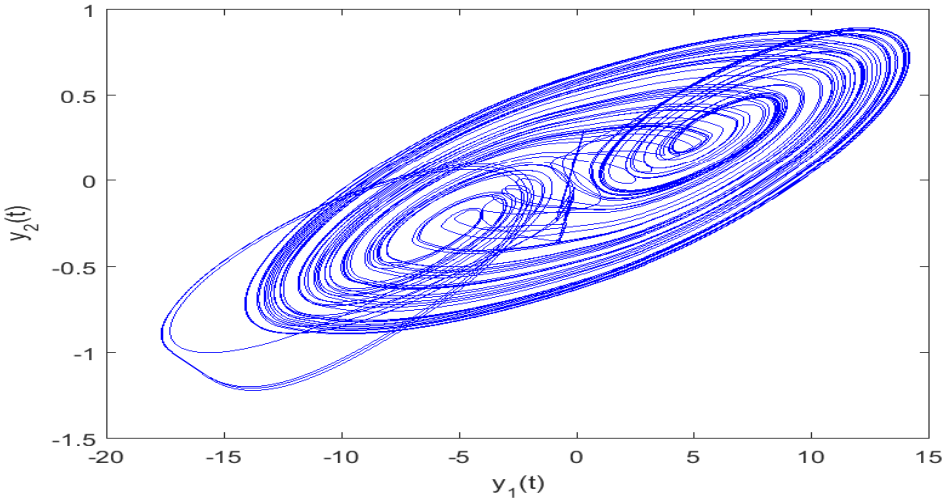

Figure 7: Chaotic behavior of slave system (29) with $u(t) = 0$.

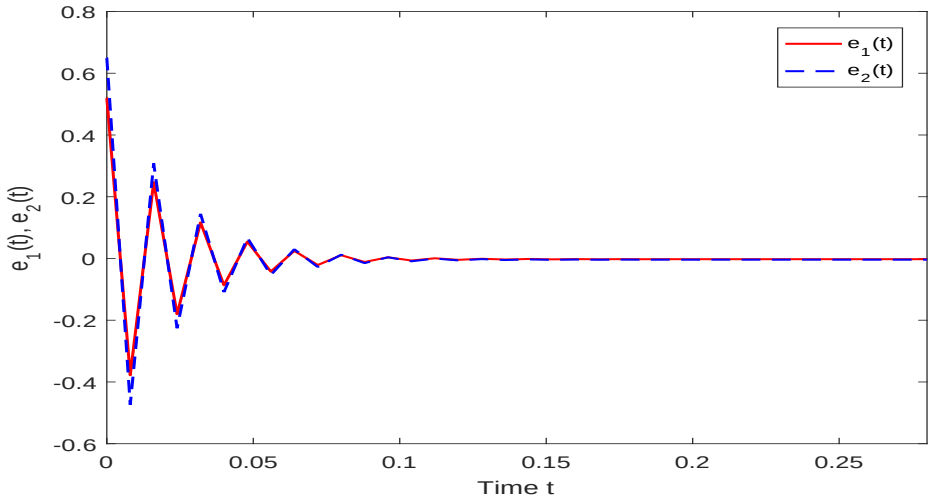

Figure 8: State responses of error system (30).

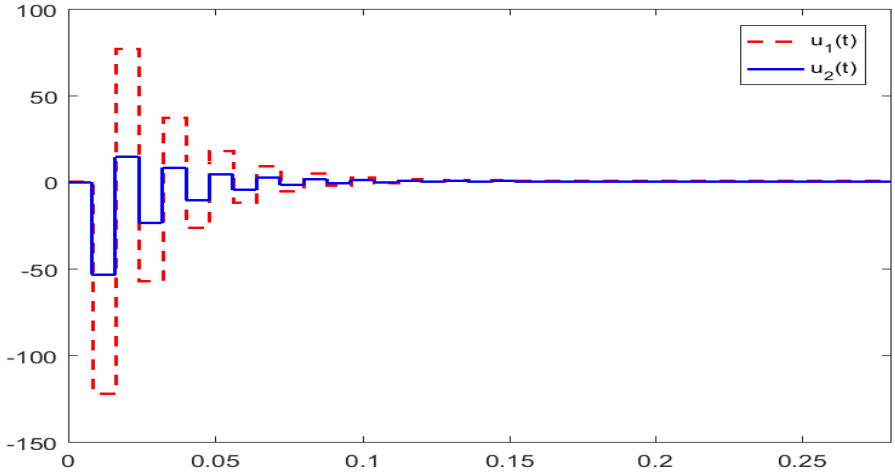

Figure 9: Control input $u(t_k)$.

Figure 10: (a) The color plain image. (b-c-d) The R, G, B components of plain image

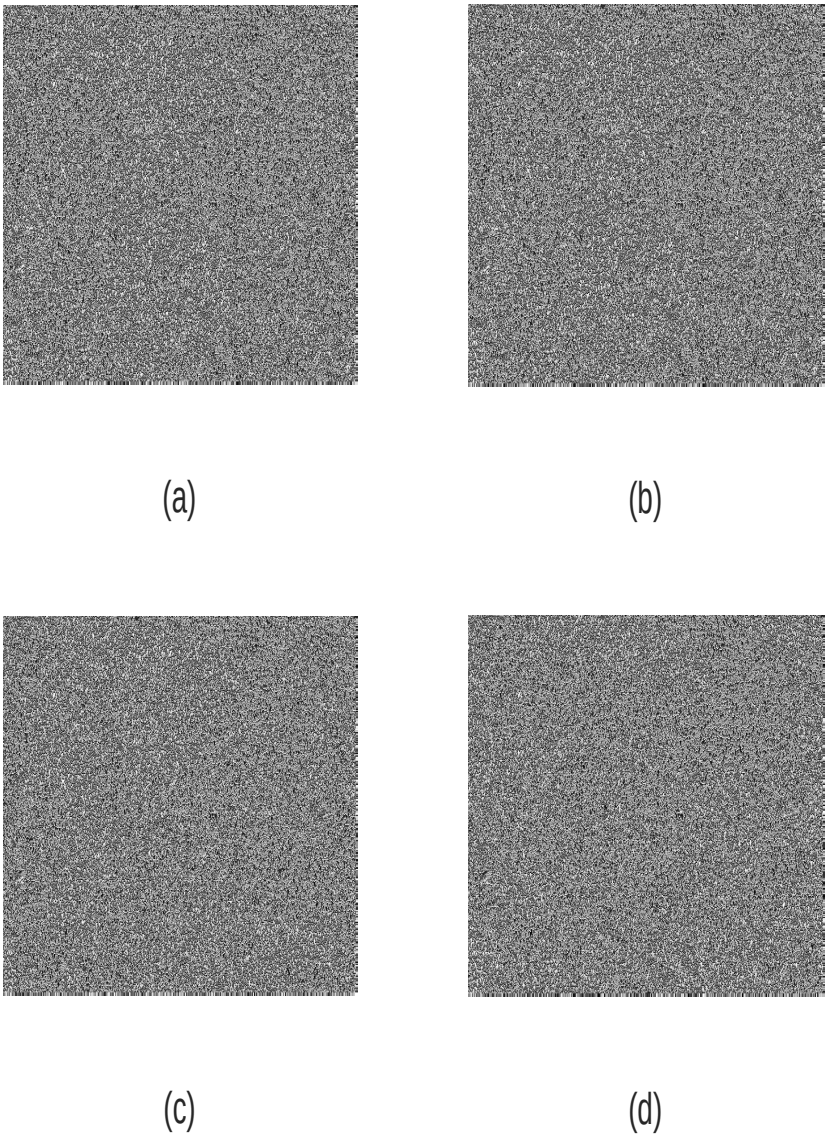

Figure 11: (a) The encrypted image. (b-c-d) the R, G, B components of encrypted image

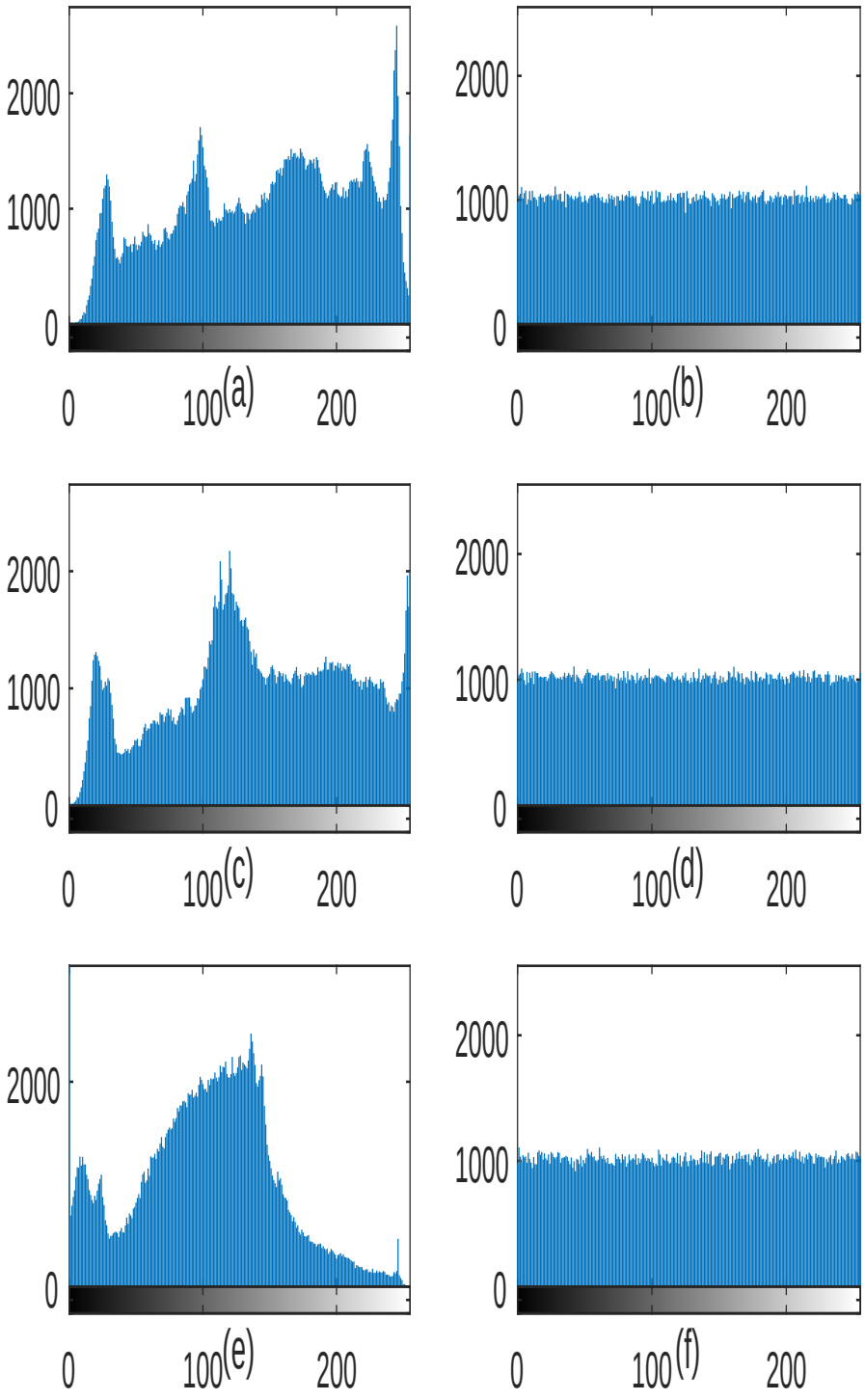

Figure 12: Histogram analysis. (a) Histogram of R components of the plain image. (b) Histogram of R components of the encrypted image. (c) Histogram of G components of the plain image.(d) Histogram of G components of the encrypted image. (e)Histogram of B components of the plain image (f) Histogram of B components of the encrypted image.